
Internal Structure of the Fly Elementary Motion Detector

Hubert Eichner



München 2011

Internal Structure of the Fly Elementary Motion Detector

Hubert Eichner

Dissertation
an der Fakultät für Biologie
der Ludwig–Maximilians–Universität
München

vorgelegt von
Hubert Eichner
aus Bad Reichenhall

München, den 30.09.2011

Erstgutachter: Prof. Dr. Alexander Borst

Zweitgutachter: Prof. Dr. Andreas Herz

Tag der mündlichen Prüfung: 13.02.2012

Contents

Summary	vii
1 Introduction	1
1.1 The Fly Visual System	3
1.1.1 Retina	4
1.1.2 Lamina	6
1.1.3 Medulla	11
1.1.4 Lobula Complex	12
1.2 Motion Detection	18
1.2.1 The Reichardt Detector	18
2 Methods	25
2.1 Preparation, Electrophysiology and Data Analysis	25
2.2 Stimulus Device	25
2.3 Stimulus Protocol and Data Analysis for Contrast and Mean Luminance Dependence	26
2.4 Stimulus Protocol for Apparent Motion Stimuli	26
2.5 Simulations	27
2.6 Parameter Fitting	30
3 Results	33
3.1 Response Strength as a Function of Mean Luminance and Contrast	33
3.2 Apparent Motion with Brightness Steps	39
3.3 Simulations and Analytical Treatment	42
3.4 Apparent Motion with Brightness Pulses	49

4 Discussion	53
4.1 Adaptation of the LMC Impulse Response	53
4.2 Four vs. Two Parallel Motion Detectors	55
4.2.1 Apparent Motion Experiments with Brightness Steps	56
4.2.2 Modeling a Motion Detector with an ON and an OFF Subunit	57
4.2.3 Apparent Motion Experiments with Brightness Pulses	58
4.3 Outlook	58
4.3.1 Biophysics of ON and OFF Separation	58
4.3.2 Characterizing the Non-Linearity	60
4.3.3 Identifying and Characterizing the Constituting Neurons	61
4.4 Concluding Remarks	63
Acknowledgments	77
Curriculum Vitae	79
Versicherung	83

Summary

Flies use visual motion information for flight control, stabilization and object tracking. However, information about local motion such as direction and velocity is not explicitly represented at the level of the retina but must be computed by subsequent motion detection circuitry. The output of these circuits can be recorded in large, direction-selective lobula plate tangential cells, that integrate over hundreds of elementary motion detectors. The computational structure of these detectors is best described by the Reichardt model, where the signals from two neighboring photoreceptors become multiplied after one of them has been delayed. However, the neural correlate of the Reichardt Detector, i.e. the identity, physiology and connectivity of the constituting cells, has escaped further characterization due to technical difficulties in recording from these small neurons.

In this thesis, I investigated the internal structure of the fly motion detection circuit by a combination of electrophysiology, computer simulations and mathematical modeling. First, I studied the effect of the mean luminance on motion detection. I found that the response strength of lobula plate tangential cells strongly depends on stimulus contrast but barely changes as a function of mean luminance. Adaptation to a new mean luminance follows an exponential decay with a time constant of several hundred milliseconds. I next investigated the structural consequences of splitting the visual input into ON and OFF components, as recently discovered in the fruit fly. The original Reichardt Detector can be refined by incorporating these findings, giving rise to two alternative structures. The 4-Quadrant-Detector consists of four independent subunits of the Reichardt type, correlating ON with ON, OFF with OFF, ON with OFF and OFF with ON signals. In contrast, the 2-Quadrant-Detector consists of two subunits only, that correlate ON with ON and OFF with OFF signals. In order to distinguish between these two models, I first stimulated flies with apparent motion stimuli consisting of a sequence of two brightness steps at neighboring locations, while recording the motion detector output in lobula plate tangential cells of the blowfly. I found strongly direction-selective responses to ON-ON and OFF-OFF sequences, but also to ON-OFF and OFF-ON sequences. At first sight, these results

seem to support the 4-Quadrant-Detector. However, I showed with simulations and an analytical treatment that the 2-Quadrant-Detector, when equipped with an appropriate preprocessing stage, is capable of reproducing such responses as well. Based on predictions from model simulations, I designed a new stimulus protocol consisting of a sequence of short brightness pulses instead of steps. For such stimuli, the 2-Quadrant-Detector does not produce significant responses to ON-OFF and OFF-ON sequences, in contrast to the 4-Quadrant-Detector. The corresponding recordings cannot be reconciled with the 4-Quadrant-Detector but are in good agreement with the 2-Quadrant-Detector.

I therefore conclude that the internal structure of the fly elementary motion detector consists of two non-interacting subunits for detecting ON and OFF motion, respectively. These results mark an important step in the ongoing dissection of the insect motion detection circuit by providing an updated model that better matches the structure and physiology of the corresponding neural hardware.

Chapter 1

Introduction

Humans and animals alike are faced with the task of deriving information about motion induced by moving objects or egomotion from the optical signals arriving at their retina. Interestingly, this information is not explicitly represented in the output signal of a single photoreceptor. It is the task of subsequent neural circuits to compute motion, its direction and speed, by analyzing the spatiotemporal dynamics of the visual stimulus as encoded by the activity of the two-dimensional array of photoreceptors.

Insects, in particular flies, have been established as a model organism in motion vision research, primarily for three reasons. First, flies show impressive capabilities in free flight, such as turning maneuvers at velocities of up to $3000^\circ/\text{s}$ and response latencies during chasing of only 30 ms (Land and Collett, 1974; Schilstra and van Hateren, 1998). Such behavior requires a highly sophisticated and specialized neural network for information processing, yet with moderate complexity to allow for these short sensory integration times. Second, insects in general offer the advantage of highly stereotyped, if not identical, sensory processing circuits across individuals or even species (Buschbeck and Strausfeld, 1997), enabling researchers to perform highly reproducible measurements on the exact same type of neuron many times and thus assigning specific functions to individual nerve cells. Third, the establishment of the fruit fly *Drosophila melanogaster* as a standard model organism in genetics has led to an unprecedented availability of genetic tools indispensable for dissecting neural circuits (for review, see Borst, 2009a). These include, most importantly, driver lines to target expression of genes in neurons of a specific type only (Brand and Perrimon, 1993). It is thus possible to express fluorescent proteins to label specific neurons for later penetration with sharp or patch-clamp electrodes (Chalfie et al., 1994; Wilson et al., 2004; Joesch et al., 2008), silence neurons by disabling vesicle release with the temperature sensitive dynamin-encoding allele *shibire^{ts}* (van der

Bliek and Meyerowitz, 1991), and excite or inhibit neurons in a temporally precise manner by optogenetic tools such as the light-activated ion channel Channelrhodopsin-2 (Boyden et al., 2005) or the light-activated chloride pump halorhodopsin (Zhang et al., 2007). Finally, it has become possible to optically record the activity of neurons with genetically encoded calcium indicators such as TN-XXL (Mank et al., 2008) or GCaMP3 (Tian et al., 2009) that might otherwise escape physiological characterization due to their small size.

To this day, the basis of insect motion detection research is the seminal work of Werner Reichardt and Bernhard Hassenstein in the 1940s and 1950s. Meeting first during Second World War, these two researchers formed an alliance to investigate motion vision by studying behavioral responses of the beetle *Chlorophanus* to visual stimuli (Borst, 2000). One outcome of this work was a mathematical model describing the process of motion detection in algorithmic terms by correlating the optical signals arriving at neighboring photoreceptors (Hassenstein and Reichardt, 1956). This correlation model, also referred to as Reichardt Detector, has since become the standard model for motion detection in insects, supported by a series of behavioral and electrophysiological studies in various insect species (see e.g. O'Carroll et al., 1996). The Reichardt Detector has gained special attention in studies of both the blowfly *Calliphora* and the fruit fly *Drosophila*. However, the neural correlate of this motion detection algorithm has remained elusive for long, due to technical difficulties in recording from the small neurons comprising the motion detection circuit.

With the advent of a wide range of genetic tools for *Drosophila*, this situation is about to change. An important first step was the recent finding by Joesch et al. (2010) that motion detection in *Drosophila* starts with splitting the visual input into two parallel channels coding for brightness increments (ON) and decrements (OFF), respectively. Further experiments by Reiff et al. (2010) showed that the extraction of the OFF component takes place in the axon terminals of neurons directly postsynaptic to photoreceptors, the so-called L2 neurons. These experiments, together with research spanning several decades on both the input stage and the output stage (the lobula plate) of the motion detection circuit, form the basis for my work.

This thesis is concerned with further dissecting the internal structure of the motion detection circuit by combining modeling and electrophysiology. First, I will introduce the fly visual system, with a focus on early sensory processing of optical signals. I will then give a description of the methods I used to carry out the experiments and model simulations, introducing a novel method for manual parameter fitting using a MIDI device to control model parameters. Subsequently, the results obtained by experiments in *Calliphora* and model simulations are presented, along with complementary results performed by my colleagues Maximilian Joesch and Bettina Schnell

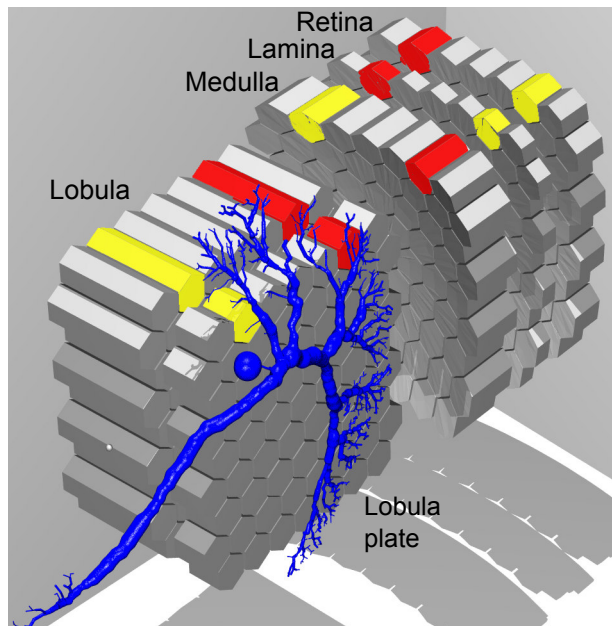


Figure 1.1: Overview of the fly visual system.

Light is detected by photoreceptors in the retina. Signals from photoreceptors with the same optical axis are transmitted to one column in the first order neuropil, the lamina. From there, neurons project to largely unknown postsynaptic partners in the second order neuropil, the medulla. Here, visual motion is detected and transmitted to large tangential neurons in the posterior region of the lobula complex, the lobula plate. As illustrated by the yellow and red labeling of columns, retinotopy is preserved throughout the visual system but is inverted by two optic chiasmata, one between lamina and medulla, one between medulla and the lobula complex. (Modified from Borst and Haag, 2002).

in *Drosophila*. The final chapter will discuss these findings, their implications and give an outlook on further dissection of the motion detection circuit of flies.

1.1 The Fly Visual System

Visual motion processing in flies starts with the detection of light by the photoreceptors R1 - R6 in the two compound eyes, followed by subsequent processing in the optic lobes underlying each eye (Fig. 1.1). Upon illumination, these photoreceptors depolarize (Hardie and Raghu, 2001) and relay information about the luminance signal to parallel processing streams in the first order neuropil, the lamina. Two of them, the lamina monopolar cells L1 and L2, transmit the major input signals to the motion detection circuit (Rister et al., 2007; Joesch et al., 2010) located in the second order neuropil, the medulla. Here, information is picked up by a largely unidentified circuit that performs motion detection. The output of this circuit is then transmitted to the third order neuropil, the lobula complex consisting of lobula and lobula plate. In the lobula plate, a set of motion-sensitive and direction-selective large-field lobula plate tangential cells (LPTCs) spatially integrates the output of presynaptic local, also called elementary, motion detectors (Single and Borst, 1998). This signal pathway is implemented on each side of the head, with extensive heterolateral connections between the two lobula plates. In addition to lobula-plate intrinsic connections, LPTCs synapse onto neck muscle motor neurons (Strausfeld and Seyan, 1985; Strausfeld et al., 1987) and onto descending neurons that project to the thoracic

compound ganglion, where they provide input to leg, neck and flight steering motor neurons (Strausfeld and Bassemir, 1985; Strausfeld and Gronenberg, 1990; Hengstenberg, 1991).

1.1.1 Retina

The compound eye of insects is a mosaic-like structure composed of hexagonally arranged ommatidia. Each ommatidium constitutes an optic apparatus with a set of photoreceptors circularly arranged below a lens. The number of ommatidia varies strongly across species, reaching more than 20.000 in large dragonflies. In the blowfly *Calliphora*, each eye consists of about 5000 ommatidia, while *Drosophila* possesses only about 750 ommatidia per eye. Each ommatidium hosts eight photoreceptors, R1 - R8, surrounded by support and pigment cells. When photons hit a specific layered structure of photoreceptor cells arranged at the central axis of an ommatidium, the light-absorbing rhabdomeres, a G-protein based signaling cascade is triggered, leading to the opening of ion channels and subsequent membrane depolarization. This process is called phototransduction (Hardie and Raghu, 2001). In *Drosophila*, R1 - R6 express the light-absorbing pigment rh1 and exhibit two peaks in their spectral sensitivity, one in the UV range and one in the green range (Stavenga, 1995). R7 and R8, in contrast, express one of the rhodopsins rh3, rh4, rh5 or rh6 in a highly regulated manner (reviewed in Mikeladze-Dvali et al., 2005). Based on their rhodopsin expression pattern, ommatidia can be divided into three different groups: in the first subtype, R7 expresses rh3 and R8 expresses rh5; in the second subtype, R7 expresses rh4 and R8 expresses rh6. The third subtype of ommatidia, the dorsal rim area, expresses rh3 in both R7 and R8; this type is found in the two most dorsal rows of the eye and is involved in orientation by detecting the oscillation plane of polarized skylight (Labhart and Meyer, 1999).

Compound eyes can be divided into three categories; the apposition eye, the optical superposition eye, and the neural superposition eye (Fig. 1.2). Apposition eyes are the most common form of compound eyes; light from a specific direction triggers neural signals in all photoreceptors of an ommatidium (the rhabdomeres of the different photoreceptors are fused to form one rhabdomere), while light from other directions is absorbed by pigment cells that optically separate the ommatidia from each other (Fig. 1.2A). This structure allows for a comparatively high spatial resolution, but is inefficient under low luminance situations because many incoming photons are lost in the pigment cells. In contrast, insects mostly active during twilight or in the night typically possess so-called optical superposition eyes, where the pigment cells that separate neighboring ommatidia from each other shorten under low light conditions, leading to photon crosstalk between neighboring ommatidia (Fig. 1.2B). This allows for efficient de-

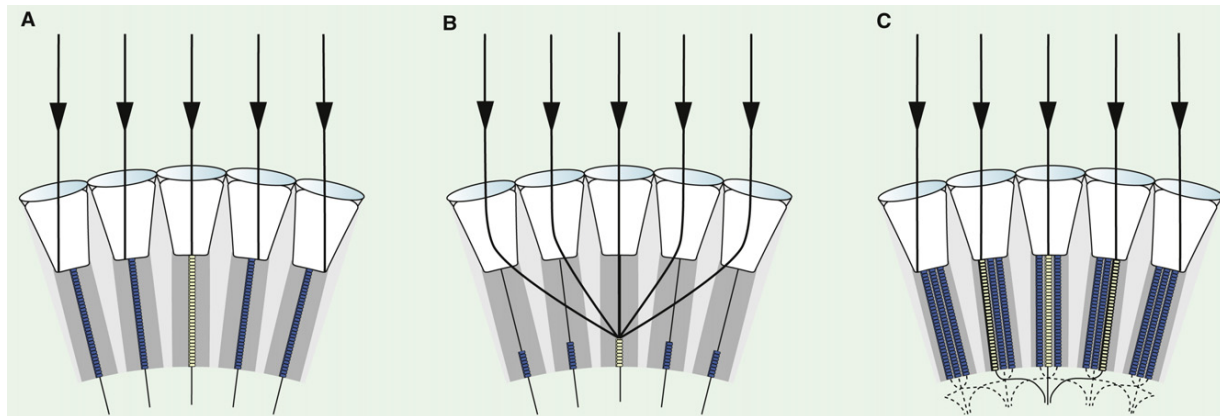


Figure 1.2: Comparison of the apposition, optical superposition and neural superposition eye.

A In the apposition eye type, light from a specific direction excites mainly one ommatidium, while the photons are absorbed in other ommatidia by the pigment cells that optically separate the ommatidia from each other. **B** In the optical superposition eye, found mainly in insects active during twilight and night, ommatidia are not optically separated from each other, and there is considerable crosstalk between ommatidia, leading to higher efficiency in detecting photons but less spatial acuity. **C** In the neural superposition eye, photo receptors in neighboring ommatidia that have the same optical axis project to the same postsynaptic partner neurons in the lamina, thus making efficient use of photons while retaining spatial acuity. (From Borst, 2009a, modified after Kirschfeld, 1967).

tection of photons, but leads to a lower spatial resolution. Optical superposition eyes are also characterized by a fused rhabdomere. The third type of compound eye, found in all diptera (including flies, e. g. *Calliphora* or *Drosophila*), is the so-called neural superposition eye. As in the apposition eye, ommatidia are separated by pigment cells, but the rhabdomeres of the eight photoreceptors are not fused; instead, the six photoreceptors R1 - R6 detect light from different optical axes. The neural superposition eye owes its name to the fact that the signals of photoreceptors in neighboring ommatidia that respond to light of the same optical axis are neuronally combined by their axons projecting to the same set of neurons in the lamina (Fig. 1.2C). As a consequence, the six photoreceptors R1 - R6 from a single ommatidium all project to different sets of lamina neurons. Photoreceptors transmit their information by releasing the neurotransmitter histamine (Hardie, 1989).

It has been shown that R1 - R6 are both necessary and sufficient for motion detection (Heisenberg and Buchner, 1977; Yamaguchi et al., 2008). R7 and R8, in contrast, bypass the lamina and project directly to the second-order neuropil, the medulla, playing an important role in color vision (Cook and Desplan, 2001; Gao et al., 2008; Yamaguchi et al., 2010).

1.1.2 Lamina

The first order neuropil, the lamina, possesses a retinotopic, columnar structure consisting of so-called lamina cartridges, groups of neurons encapsulated by glia cells (Braitenberg, 1967). Each cartridge corresponds to a specific optical axis and is constituted of 9 neurons: five lamina monopolar cells (LMC) L1 - L5, two centrifugal cells C2 and C3, an amacrine cell and the T1 cell. These cells and their connectivity have been thoroughly studied in *Drosophila* using electron microscopy (Meinertzhagen and O'Neil, 1991; Takemura et al., 2008). L1 - L3 and the amacrine cell receive direct histaminergic synaptic input from photoreceptors, whereas L4, L5 and the T1 cell receive indirect input only. L2 provides a feedback synapse onto photoreceptors and a synapse onto L4. The amacrine cell connects to the T1 cell. L4 connects to L2 in the same cartridge but also projects to two neighboring posterior lamina cartridges where it synapses onto L2 cells. It also shows similar collaterals in front-to-back direction in its terminal region in the medulla. L1 and L2 have been shown to be electrically coupled by gap junctions (Joesch et al., 2010). C2 and C3, in contrast, are feedback neurons projecting from the medulla to the lamina.

L1 - L5 and T1 all project to the medulla but arborize in different layers (Fig. 1.3; Fischbach and Dittrich, 1989; Takemura et al., 2008). It has been proposed that L1 and L2 form the input to different motion detection pathways (Bausenwein et al., 1992; Bausenwein and Fischbach, 1992; Katsov and Clandinin, 2008). Importantly, a behavioral study by Rister et al. (2007), later confirmed by electrophysiological recordings by Joesch et al. (2010), showed that in *Drosophila*, rescuing histamine receptor function in L1 and L2 but not in other lamina neurons is both necessary and sufficient for motion detection. Therefore, these cells are assumed to constitute the gateway to the motion detection circuit. The electrophysiological characterization of these cells has been performed mainly in *Calliphora*, with only few studies having addressed *Drosophila* (but see Zheng et al., 2006, 2009). While these studies and the similarity of electro-retinograms in *Calliphora* and *Drosophila* indicate similar LMC response properties in these species, no quantitative electrophysiological comparison has been carried out yet. Buschbeck and Strausfeld (1997) compared the anatomy and stratification patterns of lamina neurons across taxa and found a very high degree of evolutionary conservation; these results suggest that not only anatomy but also the physiology of the motion detection circuit bears close resemblance between *Calliphora* and *Drosophila*.

The two largest lamina monopolar cells by diameter, L1 and L2, seem to receive most synaptic input from R1 - R6 (Meinertzhagen and Sorra, 2001). Histamine release by photoreceptors leads to the opening of chloride channels in the dendrites of these cells and subsequent

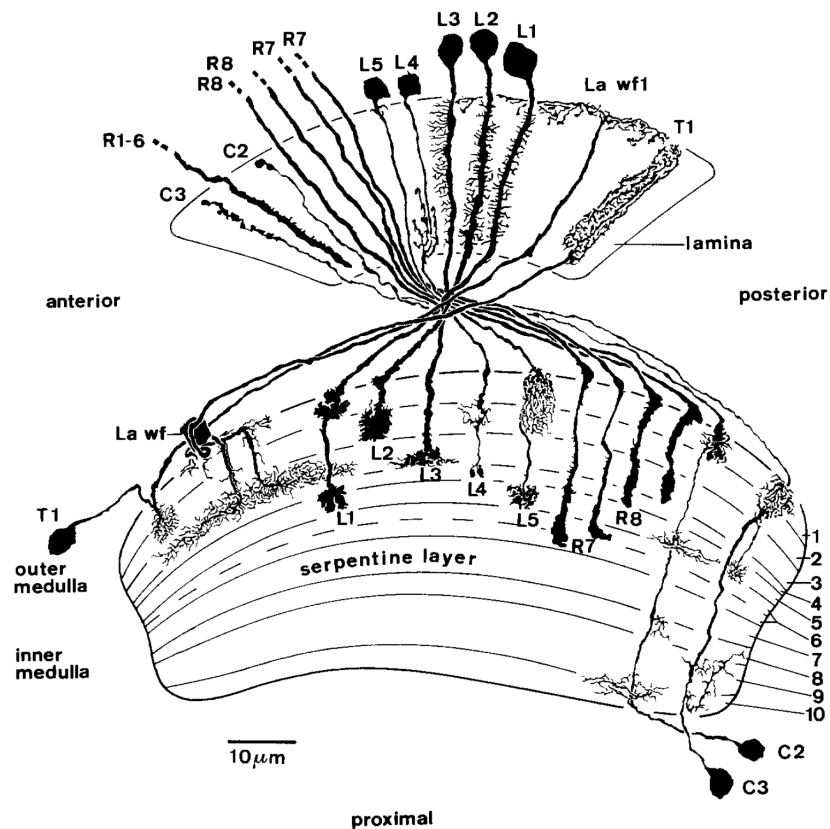


Figure 1.3: Cell types of the retina and the lamina and their projections to the medulla.

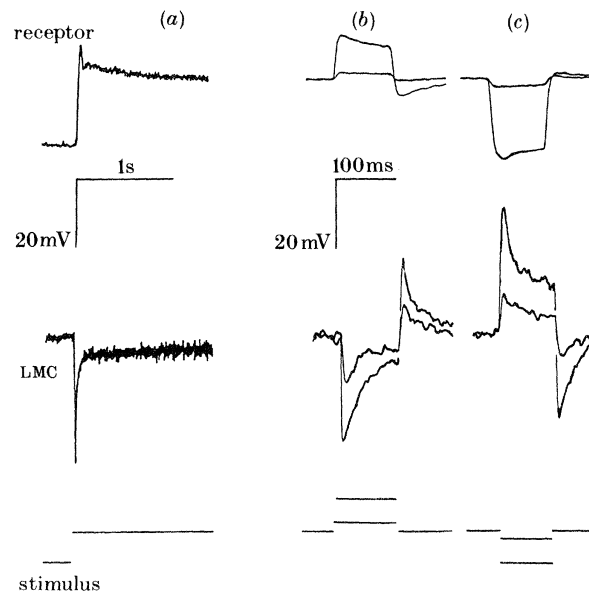
Anatomical reconstructions of retina and lamina cell types from Golgi stainings in *Drosophila*. Each of the depicted neuron types occurs once in each lamina and medulla column. R1 - R6 project into the lamina, where they synapse onto L1 - L3 and the amacrine cell (not shown). The lamina cells L1 - L5 and T1 then project into the medulla, arborizing in different layers. In contrast, the photo receptors R7 and R8 bypass the lamina and project directly into the medulla. (From Fischbach and Dittrich, 1989).

hyperpolarization (Hardie, 1989). L1 and L2 have been studied extensively in *Calliphora* with sharp electrode recordings in their dendrites (Järvilehto and Zettler, 1971; Srinivasan et al., 1982; Laughlin et al., 1987; van Hateren, 1992a; for review, see Laughlin, 1994). Because high-impedance microelectrodes are required to record from these cells, it is not possible to simultaneously fill them with dye to determine which cell one is recording from. It is commonly assumed that, at the location of recording in their dendrites, these two cell types exhibit the same response properties.

Accordingly, these cells respond with hyperpolarizations to brightness increments and depolarizations to brightness decrements (Fig. 1.4). Their spatial receptive field is the same or

Figure 1.4: Comparison of photoreceptor and LMC responses to brightness steps.

Photoreceptors (upper row) and LMCs (middle row) respond to luminance steps (bottom row) depending on the amplitude of the stimulus. However, they differ in the sign of their responses: photoreceptors depolarize for ON steps and hyperpolarize for OFF steps, while LMCs hyperpolarize for ON steps and depolarize for OFF steps. Furthermore, LMCs are characterized by much more transient responses that decay back towards the original membrane potential quickly following a the brightness step. Nonetheless, they do not act as pure high-pass filters; instead, a certain DC component remains in the LMC signal. (From Laughlin et al., 1987).



even narrower than that of the corresponding photoreceptors, indicative for lateral inhibition (Järvilehto and Zettler, 1973; Srinivasan et al., 1982). In contrast to photoreceptors, LMC responses were found to have a very transient nature, resembling a high-pass filtered version of the luminance signal. They respond to brightness steps with an initial positive (for a brightness decrement) or negative (brightness increment) peak of their membrane potential that subsequently decays back towards, but not entirely reaching, the previous membrane potential baseline level (Fig. 1.4; for review, see Laughlin, 1994). The LMC response therefore contains a certain DC component as well. Thus, the voltage signal of the LMC dendrite contains not only information about brightness changes but about the absolute brightness as well.

The stimulus-induced responses of LMCs can, in principle, be predicted by convolving the stimulus with a (static) LMC impulse response (van Hateren, 1992a) or, as an approximation, by high-pass filtering the stimulus. One could therefore refer to the high-pass characteristics of LMCs as *adaptation* to a new mean luminance. In this thesis, however, I am going to use the term adaptation in the LMC context in a different manner, namely adaptation of the LMC *impulse response*. Both the spatiotemporal profile and the amplitude of LMC impulse responses are subject to strong adaptation to the mean luminance level (Fig. 1.5; Laughlin et al., 1987; van Hateren, 1992a,b). The spatiotemporal impulse response properties can, in fact, be nicely modeled by assuming the impulse response adapts to the stimulus statistics such that it maximizes information transmission under different signal-to-noise regimes (van Hateren, 1992c). In addition, the amplitude of the impulse response is subject to scaling: LMCs approximately encode stimulus contrast, that is, the ratio of brightness steps to the prevailing

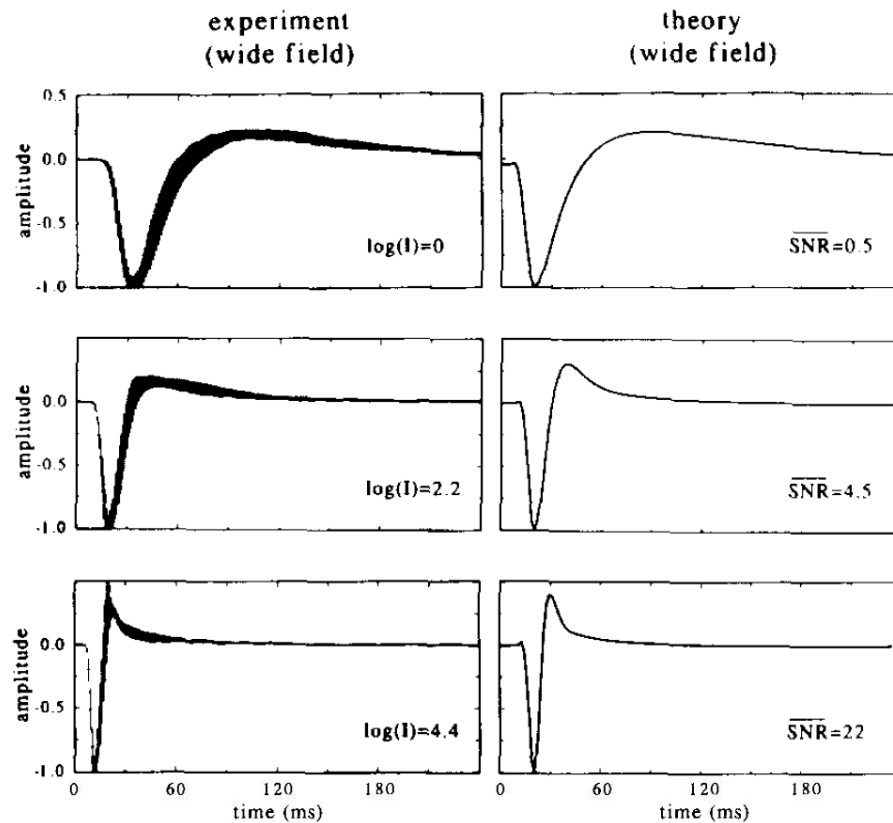


Figure 1.5: LMC impulse responses as predicted by information maximization.

Measured (left column) and estimated (right column) impulse responses of LMCs to short, wide field brightness pulses under different luminance (signal-to-noise) conditions. Theoretical predictions are computed by maximizing information transmission from moving natural images at different light levels. (From Laughlin, 1994 after van Hateren, 1992b).

mean luminance (Laughlin et al., 1987). As a consequence, doubling both the mean luminance and the amplitude of a brightness step stimulus leads to approximately the same response strength in an adapted LMC, whereas a linear filter with constant amplitude would give a response twice as strong. To my knowledge, the temporal properties of this adaptation process - i.e. on what time scale does adaptation of impulse response amplitude and temporal profile occur - have not been analyzed yet to an extent that a corresponding model for LMCs exists. Instead, previous publications concerned with modeling insect motion detection estimated LMC responses by convolving the stimulus with static impulse responses (Dror et al., 2001; Lindemann et al., 2005; Spavieri et al., 2010; Tuthill et al., 2011).

Interestingly, all electrophysiological recordings were performed in LMC dendrites, and it was commonly believed that these response properties apply to the output signals of LMCs as well. However, in 2010, Reiff et al. measured calcium signals with genetically encoded calcium indicators in *Drosophila* L2 axon terminals in response to gratings and brightness steps. The changes in calcium concentration, indicative for the actual synaptic vesicle release of these cells, showed only small calcium decreases in response to ON steps (dendritic hyperpolarizations), but strong calcium increases in response to OFF steps (dendritic depolarizations) were observed.

Surprisingly, however, the time constant of the calcium response decay was much larger (about 2.1 s) than estimated from electrophysiological recordings in these cells. Similar temporal properties have been recently observed in axon terminals of L1 (Clark et al., 2011).

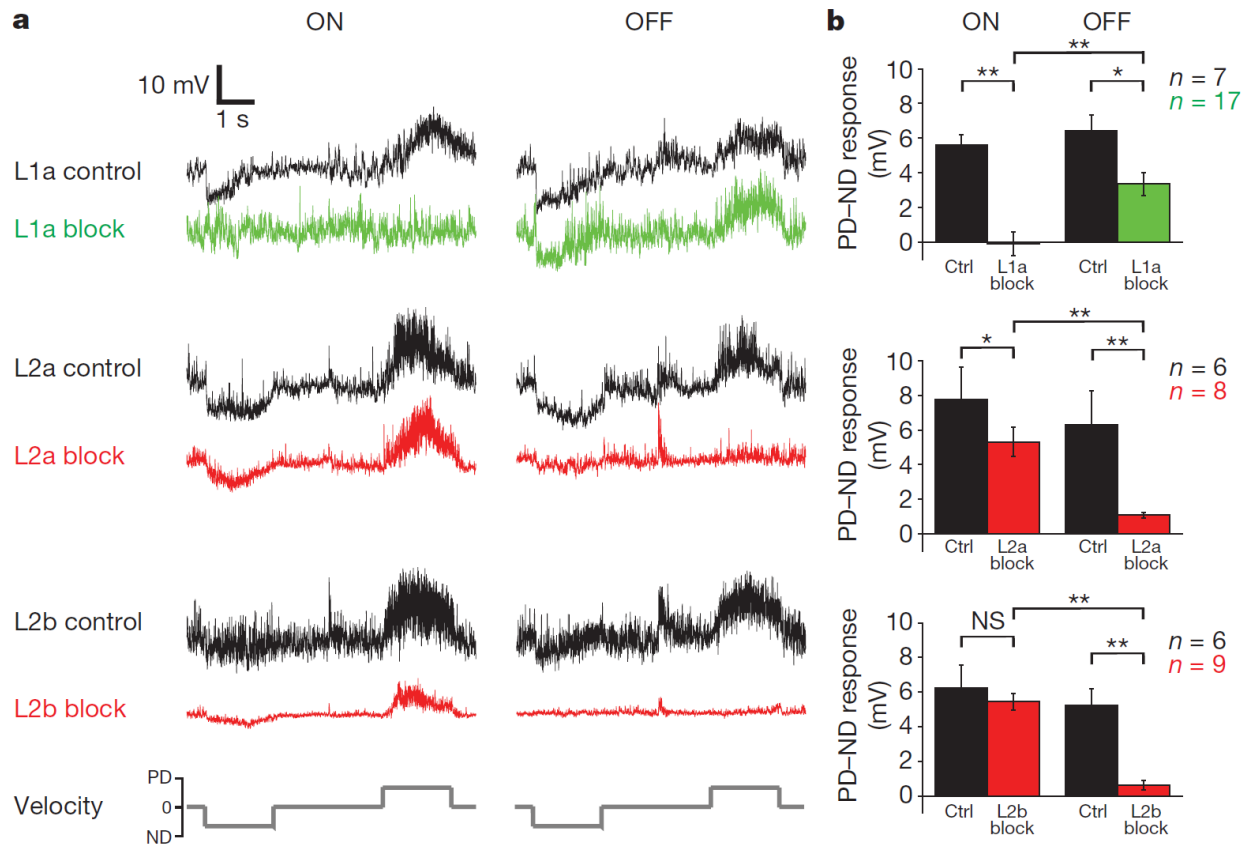


Figure 1.6: L1 and L2 split the visual input into its ON and OFF components.

Three different *Drosophila* driver lines (L1a, L2a and L2b) were used to express in L1 or L2 a temperature-sensitive allele of the dynamin-encoding gene *shibire*, which suppresses synaptic output for higher temperatures by inhibiting vesicle recycling (Kitamoto, 2001). For permissive temperatures, that is, when endocytosis is functional, LPTCs respond to both moving ON and OFF edges in both the preferred direction and null direction of the cell. When the synaptic output of L1 is suppressed by increasing the temperature, the motion detection circuit no longer detects the movement of ON edges but responds to OFF edges in a manner similar to the control condition. Blocking L2 synaptic output, in contrast, suppresses the detection of moving OFF edges. (From Joesch et al., 2010).

A recent study by Joesch et al. (2010) has investigated the role of L1 and L2 in motion detection. *Drosophila* flies were stimulated with moving ON or OFF edges while simultaneously recording responses in motion-sensitive and direction-selective LPTCs, which integrate over a large array of presynaptic elementary motion detectors. In wild-type flies, clear direction-

selective responses to both moving ON and OFF edges can be observed (Fig. 1.6). When blocking the synaptic output of L1 cells, only responses to moving OFF edges could be observed, but not to ON edges. Accordingly, blocking the synaptic output of L2 removed LPTC responses to moving OFF edges, while retaining the responses to ON edges. This shows that the visual input is transmitted into different ON and OFF channels already in cells directly postsynaptic to photoreceptors. These findings are in agreement with optical recordings by in L2 axon terminals. The OFF extraction seems to occur in L2 (Reiff et al., 2010) by rectifying voltage-activated calcium channels, while the location and biophysics of the ON rectification are currently unknown (Clark et al., 2011).

In summary, L1 is necessary to transmit ON signals, while L2 transmits OFF signals to the motion detection circuit; both cells show filter properties resembling a high-pass filter but retain a certain DC component indicative for the absolute luminance. These results do not preclude a role of L4 in motion detection, which is postsynaptic to L2 in the same cartridge and provides input to L2 cells in neighboring cartridges.

1.1.3 Medulla

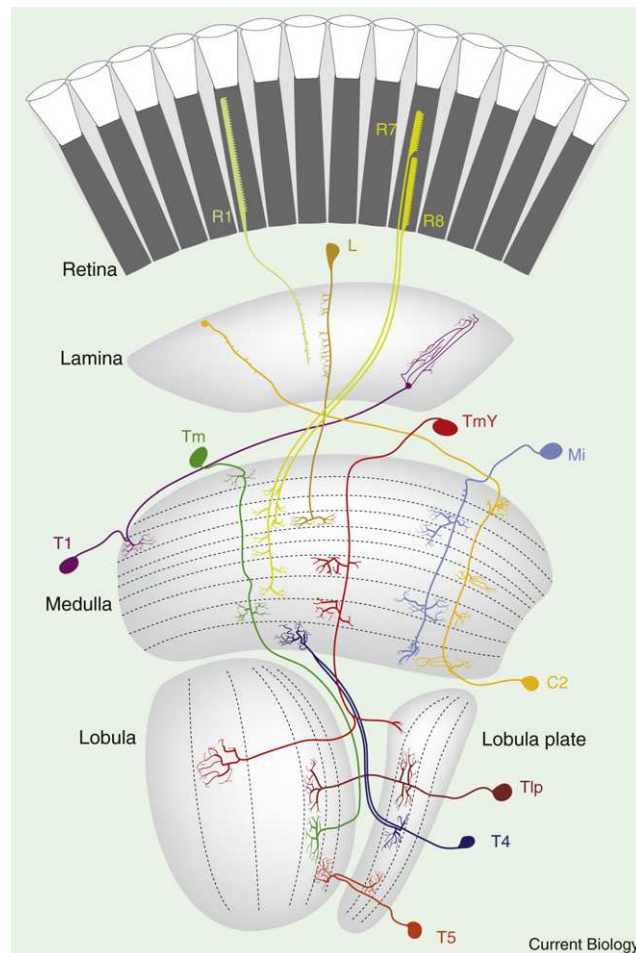
The second order neuropil, the medulla, again exhibits a retinotopic, columnar organization similar to the lamina. Each column can be divided into ten layers, M1 - M10. The lamina neurons ramify in different layers of the medulla (Strausfeld, 1976; Fischbach and Dittrich, 1989; Takemura et al., 2008). Most notably, L2 exhibits axonal ramifications in layer M2, while L1 projects to two different layers, M1 and M5 (Fig. 1.3). Each column is comprised of approximately 60 neurons. As the next neuropil, the lobula complex, contains large, motion sensitive and direction selective cells in its posterior part, the lobula plate, motion computation is assumed to take place in the medulla and, possibly, the lobula.

Anatomical studies (Strausfeld, 1976; Fischbach and Dittrich, 1989) have lead to a classification of medulla neurons into medulla intrinsic (Mi) neurons contained entirely within the medulla, transmedullary neurons (Tm) connecting the medulla to the lobula, Y-shaped transmedullary neurons (TmY) connecting the medulla to both the lobula and the lobula plate, and T4 cells connecting the innermost layer M10 with the lobula plate (Strausfeld and Lee, 1991). In addition, T5 cells connect the lobula to the lobula plate, providing another possible pathway for motion detection (Fig. 1.7).

Based on studying co-stratification of different cell types in specific layers of the medulla and the lobula (Bausenwein et al., 1992), two parallel motion detection pathways were proposed; the L1 pathway, involving L1, Mi1, and T4 cells in layer M10, and the L2 pathway, involving

Figure 1.7: Cell types in the optic lobes.

Each column in the medulla consists of about 60 different neurons, of which a small subset is shown in the figure on the right. These cells can be classified according to their projection pattern into medulla-intrinsic neurons (Mi cells), transmedullary neurons connecting the medulla to the lobula (Tm cells), transmedullary Y neurons projecting from the medulla to both the lobula and the lobula plate (TmY cells), and T cells that project from either the medulla or the lobula to the lobula plate, with their cell bodies located posterior to the lobula complex. (From Borst, 2009a, modified after Fischbach and Dittrich, 1989).



L2, Tm1 and T5 cells. Indeed, 2-deoxyglucose labeling provided certain evidence that these pathways are involved in motion detection (Buchner et al., 1984; Bausenwein et al., 1992). However, these propositions remain speculation since medulla cells are very small and hard to record from, and only little data from short recordings and/or unidentified columnar neurons exist (DeVoe, 1980; Gilbert et al., 1991; Douglass and Strausfeld, 1995, 1996, 1998).

1.1.4 Lobula Complex

The third order neuropil, the lobula complex, consists of two parts, the anterior lobula and the posterior lobula plate, both exhibiting a retinotopic, columnar structure. The lobula has seen only little attention in physiological studies in flies. It consists of six layers (Strausfeld, 1989); Buchner et al. (1984) observed 2-deoxyglucose-labeling of up to three layers (depending on the stimulus) in *Drosophila* during stimulation with moving gratings or flicker.

In contrast, the lobula plate has been studied for decades using imaging and electrophysiol-

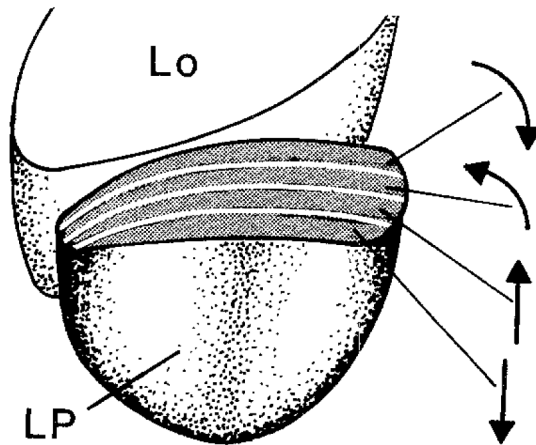


Figure 1.8: Layered structure of the lobula plate.

Using 2-deoxyglucose labeling in *Drosophila*, four different layers can be observed in the lobula plate (LP), depending on the stimulus direction. This labeling indicates that elementary motion detectors with different preferred directions project into specific layers, in the order front-to-back, back-to-front, upward, downward from the anterior to the posterior lobula plate. (From Buchner et al., 1984).

ogy (for review, see Borst and Haag, 2002). It can be separated into four different layers based on 2-deoxyglucose labeling in *Drosophila*, each layer being active for a different motion direction (Fig. 1.8) of a moving stimulus (Buchner et al., 1984; Bausenwein et al., 1992; Bausenwein and Fischbach, 1992).

The retinotopically arranged columns of the lobula plate are thought to provide motion detector input to lobula plate tangential cells (LPTCs) spanning a large area of or even the whole lobula plate (Egelhaaf et al., 1989; Single and Borst, 1998; Spalthoff et al., 2010). This input is presumably transmitted via T4 and T5 cells. Both T4 and T5 can be divided into four subclasses (T4a - T4d and T5a - T5d), respectively (Fischbach and Dittrich, 1989), based on which of the four layers of the lobula plate the subclass projects to (T4a and T5a terminate in the most anterior, T4d and T5d in the most posterior layer). T5 has been reported to respond in a direction-selective way, while T4 responded only weakly direction-selective (Douglass and Strausfeld, 1995, 1996). In addition, Strausfeld and Lee (1991) found a chemical synapse between a T4 cell and an HS cell in electron micrographs. There is strong indication that the information from the motion detection circuit is transmitted onto LPTCs by both excitatory cholinergic and inhibitory GABAergic input (Brotz and Borst, 1996; Single et al., 1997; Raghu et al., 2007, 2009, Fig. 1.9). As will be discussed in the following chapter, such input is in agreement with theoretical predictions from the Reichardt Detector.

In *Calliphora* and *Musca*, the lobula plate contains about 60 individually identifiable LPTCs. Most of them have large and complex receptive fields that arise from both the spatial integration over many presynaptic elementary motion detectors and from connections with other LPTCs. These receptive fields usually match a specific type of optic flow (Krapp and Hengstenberg, 1996; Krapp et al., 1998; Wertz et al., 2009) such as translational or rotational movements. They can be roughly divided into cells responding preferentially to vertical motion (e. g. VS1 -

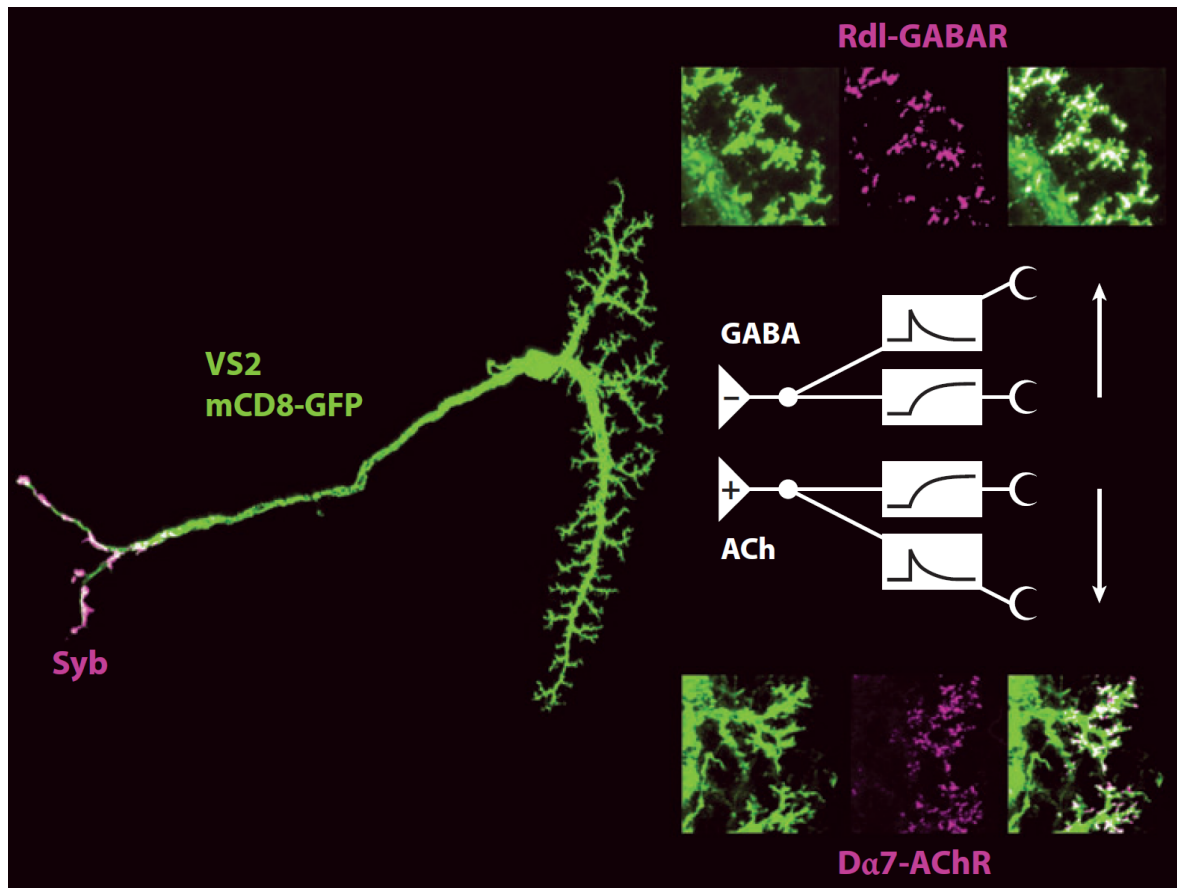


Figure 1.9: Cholinergic and GABAergic input to LPTCs.

On the left, a *Drosophila* mCD8-GFP labeled VS2 cell is depicted in green. On the right, co-localization of DsRed-labeled synaptic receptor proteins (Rdl for GABA and $D\alpha 7$ for acetylcholine) with the dendrites is shown, suggesting both inhibitory and excitatory input to LPTCs. The white insets show the assumed processing stages according to the Reichardt Detector giving rise to the inhibitory and excitatory input. (From Borst et al., 2010, based on Raghu et al., 2007, 2009).

VS10, V1, V2) or horizontal motion (e. g. HSS, HSE, HSN, vCH, dCH, H1, H2), responding with an increase in activity to motion in one direction, their preferred direction (PD), and a decrease of activity to motion in the opposite, their null direction (ND). Different LPTCs respond to motion with changes in their membrane potential, their firing rate, or both. A subset of LPTCs, the so-called Fd cells, have been shown to respond to motion of small objects irrespective of background motion (Egelhaaf, 1985a,b). LPTC responses to a moving stimulus depend not only on the local direction but also on contrast (Warzecha and Egelhaaf, 2000; Borst, 2003b) and size (Hausen, 1984; Lenting et al., 1984; Haag et al., 1992) of the pattern.

For both parameters, saturation effects can be observed.

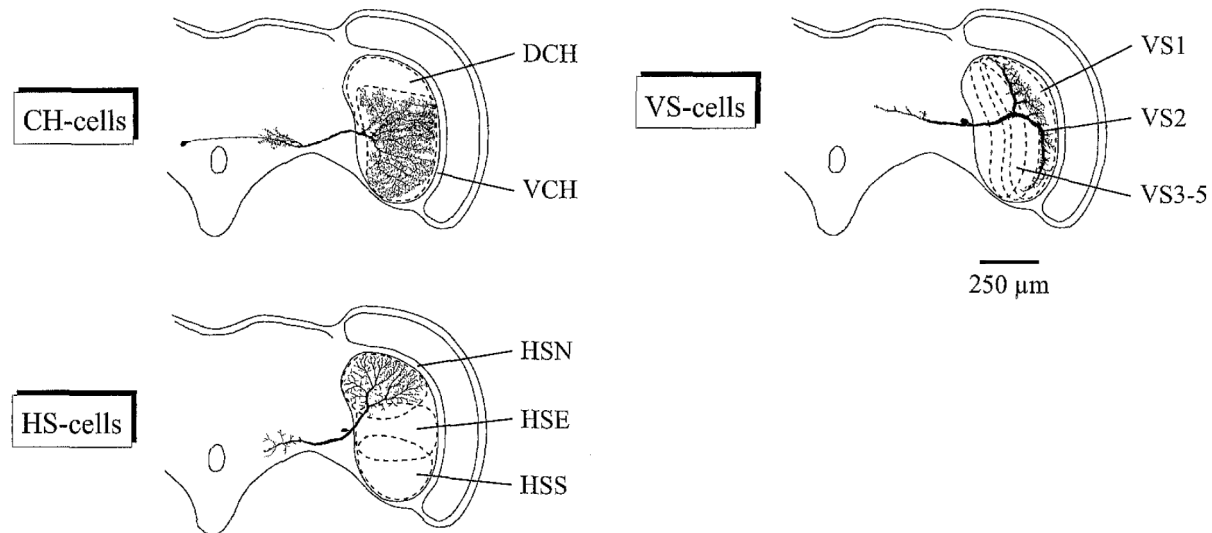


Figure 1.10: Different positions of LPTC dendrites within the lobula plate.

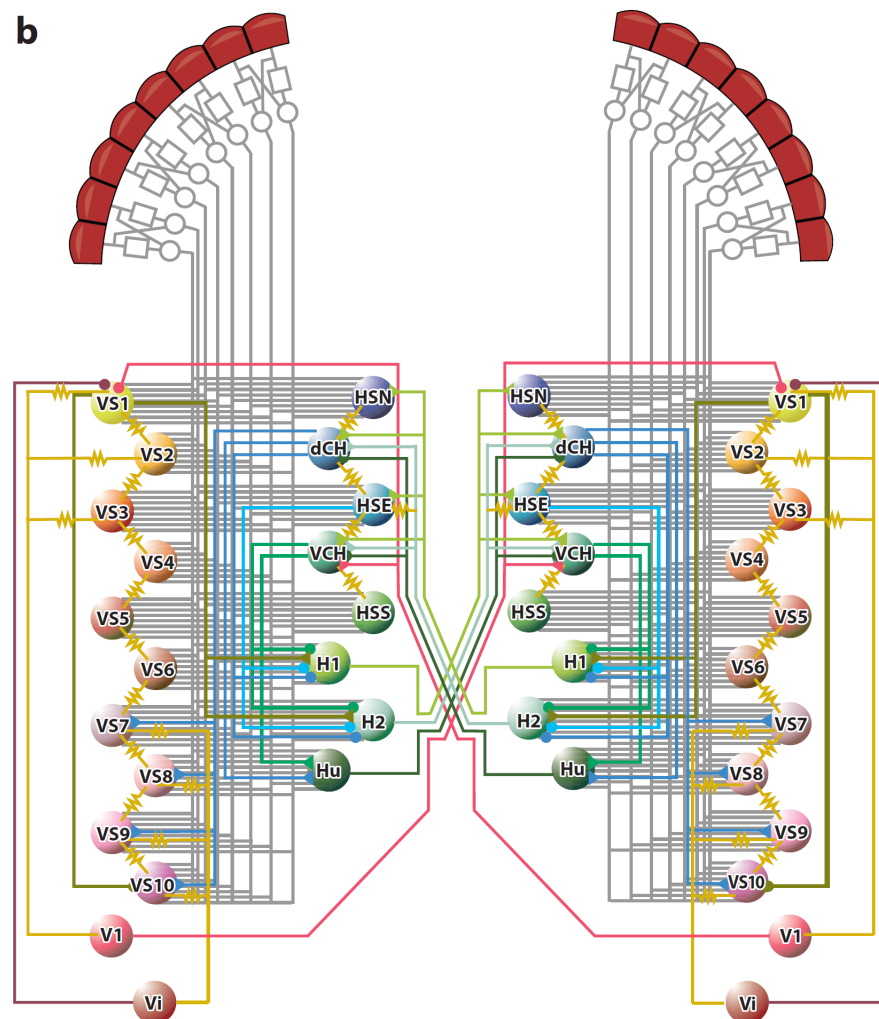
The location of three different classes of cells (CH, HS, VS) within the lobula plate is shown in a schematic cross-section through the head of a fly. The anatomy of one representative of each class is drawn, and the dendritic fields of other members of the same class are indicated with dashed lines. (Modified from Borst and Haag, 1996).

Figure 1.10 shows the location of different LPTCs within the lobula plate. Due to the columnar, retinotopic organization of the presynaptic elementary motion detectors, the angular extent of LPTC receptive fields can be approximately predicted from the location and size of their dendritic tree within the lobula plate. However, the receptive field of many LPTCs is shaped not only by motion detector input but also by extensive lobula-plate-intrinsic connections. For instance, Haag and Borst (2004) and Elyada et al. (2009) have shown that VS cells receive both dendritic motion detector input and axonal gap-junction mediated input from other VS cells, leading to different (broader) axonal than dendritic receptive fields within the same cell. Other LPTCs such as dCH and vCH presumably do not receive direct motion detector input at all but are dendro-dendritically coupled with HS cells via gap junctions (Farrow et al., 2006).

LPTCs are in general easily accessible for recordings; their receptive fields and the connectivity scheme within the lobula plate and between the two heterolateral lobula plates have been studied in *Calliphora* in great detail in the last forty years, giving rise to a complex, yet incomplete circuit diagram (Fig. 1.11; for review, see Borst et al., 2010). LPTCs were found

Figure 1.11: Connectivity scheme of the lobula plate network.

This figure illustrates a subset of the LPTCs in *Caliphora* and their currently known connectivity via gap junctions (yellow, resistors), inhibitory (circles) and excitatory (triangles) synapses. In addition to lobula-plate-intrinsic connectivity, several connections between the two heterolateral lobula plates have been found. Furthermore, LPTCs receive input from presynaptic local motion detectors (depicted in gray). (From Borst et al., 2010).



to be connected to each other in numerous ways, via gap junctions, excitatory and inhibitory synapses; several spiking LPTCs project to other LPTCs in the contralateral lobula plate.

LPTCs are thought to play a major role in visual course control of the fly. First, the response properties of LPTCs are in good agreement with motion-driven behavior (Götz, 1975; Hausen, 1982; Borst and Bahde, 1988), although this rather reflects that both are based on the same type of motion detection circuit. Second, the *Drosophila* mutant *optomotor-blind*^{H31} has a phenotype where the whole lobula plate is missing; this mutant shows almost no optomotor response, i.e. behavioral responses to visual stimuli (Heisenberg et al., 1978). Third, various lesion experiments in the lobula plate lead to modified and reduced optomotor responses (Geiger and Nässel, 1982; Hausen and Wehrhahn, 1983). Fourth, as mentioned before, LPTCs project both onto neck muscle motor neurons and onto descending neurons that, in turn, provide input

to neck muscle, flight steering and leg motor neurons.

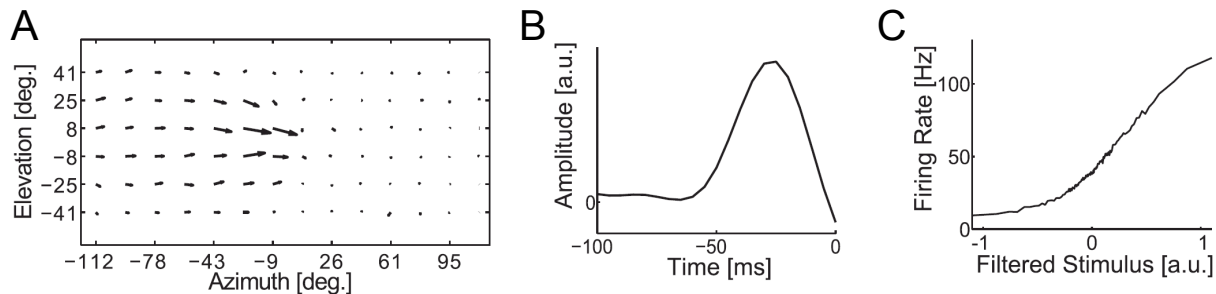


Figure 1.12: Spatial and temporal receptive field properties of H1.

H1 firing rates can be predicted by a so-called Linear-Nonlinear model, a cascade of a spatiotemporal filter and a static non-linearity. The stimulus is convoluted with the spatiotemporal filter, and the result is fed through a non-linearity to give a firing rate estimate. The optimal spatiotemporal filter found by reverse correlation techniques is space-time separable. The figure depicts **A** the spatial and **B** the temporal component of the filter of an H1 cell receiving motion sensitive input from the left side. The arrows in the spatial receptive field indicate the local preferred direction. **C** The relationship between filter output and firing rate. (Modified from Weber et al., 2010).

One of the most studied cells in neurobiology is arguably the horizontally sensitive spiking lobula plate neuron H1 (Hausen, 1984). Its dendrites cover almost the whole lobula plate, and accordingly, it responds to motion in almost the complete ipsilateral hemisphere (Fig. 1.12A). H1 is mainly excited by back-to-front motion (for a detailed analysis of the spatiotemporal receptive field of H1, see Weber et al., 2010); this information is then transmitted via a long axon to the contralateral lobula plate, where it synapses onto cells of the horizontal system, its axonal arborizations also covering the complete lobula plate. H1 has been used as a model neuron for researching information coding in general (Bialek et al., 1991; Fairhall et al., 2001; Spavieri et al., 2010) due to the possibility to record its activity for long periods of time (up to several days). In this thesis, I will use H1 to study the motion detection circuit in flies mainly due to the simplicity in recording neural responses for extended periods of time, as required for white-noise experiments and for scanning large stimulus parameter spaces. It must be noted, however, that it is not known whether H1 receives direct synaptic input from the motion detection circuit or indirectly from other motion-sensitive LPTCs. Nonetheless, its response properties with regard to stimulus parameters such as wavelength, angular velocity and contrast are similar to those of all other LPTCs (Haag et al., 2004).

1.2 Motion Detection

The large and often complex receptive fields of LPTCs have been shown to arise from both the spatial integration over many presynaptic local motion detectors and the connectivity between different LPTCs. Neurons that exhibit local motion detection, that is, direction-selective cells with comparably small receptive fields, have been observed in many different species: in retinal ganglion (Barlow et al., 1964) and starburst amacrine cells (Euler et al., 2002) in rabbits, salamanders and mice; in complex cells in area V1 of the visual cortex in cats (Hubel, 1959; Hubel and Wiesel, 1959), and in area MT (Dubner and Zeki, 1971; Albright et al., 1984) of macaques. Nonetheless, local motion detection has probably been characterized best in flies, with a model introduced more than 6 decades ago, the correlation-type or Reichardt detector (Hassenstein and Reichardt, 1956).

1.2.1 The Reichardt Detector

Introduction

The Reichardt Detector was originally proposed to model the visually induced turning tendency of the beetle *Chlorophanus* walking on a spherical Y-maze made of straws (Hassenstein and Reichardt, 1951, 1956; Reichardt, 1961). It has since seen extensive use in modeling behavioral and electrophysiological responses of insects to motion (Borst et al., 2010) as well as, in adapted forms, in vertebrate vision and psychophysics (Sekuler et al., 1990; Zanker, 1996). While there are other classes of motion detection models such as the gradient detector (reviewed in Borst, 2009b), the motion-sensitive responses measured in insects speak in strong favor of the Reichardt Detector.

In its most basic form, the Reichardt Detector (Fig. 1.13) consists of two mirror-symmetrical subunits, the so-called half-detectors. Each half-detector computes motion by multiplying the output signals of two neighboring photoreceptors after one of them has been low-pass filtered. The output signals of both half-detectors are finally subtracted to enhance direction-selectivity. The reasoning behind this structure can be summarized as follows. First, motion detection requires at least two spatially separate input lines, i.e. photoreceptors - it is impossible to infer the direction of a moving object from the observation of a single point in space, only, as such an observation is invariant to rotations of the stimulus around the point of observation. Second, the structure of a motion detection mechanism must be asymmetric with regard to how the signals from two input lines are processed - otherwise, the two input lines could be

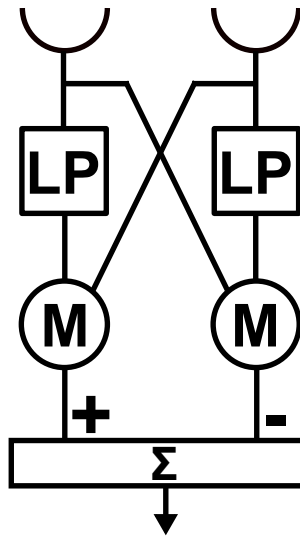


Figure 1.13: The Reichardt Detector.

The Reichardt Detector is symmetrically structured, consisting of two so-called half-detectors. In its most basic form, each half-detector computes motion by multiplying the output of two neighboring photoreceptors after one of them has been delayed by a low-pass filter. This operation is performed twice in a mirror-symmetrical manner, and the two results are finally subtracted to enhance direction selectivity.

exchanged without a change in the response, i.e. direction-selectivity is lost. This asymmetry is implemented by differential filtering of the two input lines (in the most basic form, only one input signal is low-pass filtered before the two signals are multiplied). Third, the two signals must be combined by a non-linear operation, a multiplication in the case of the Reichardt Detector - otherwise, the time average of the response to a moving sine grating would be 0 (Appendix A in Buchner, 1976).

Experimental Support for the Reichardt Detector

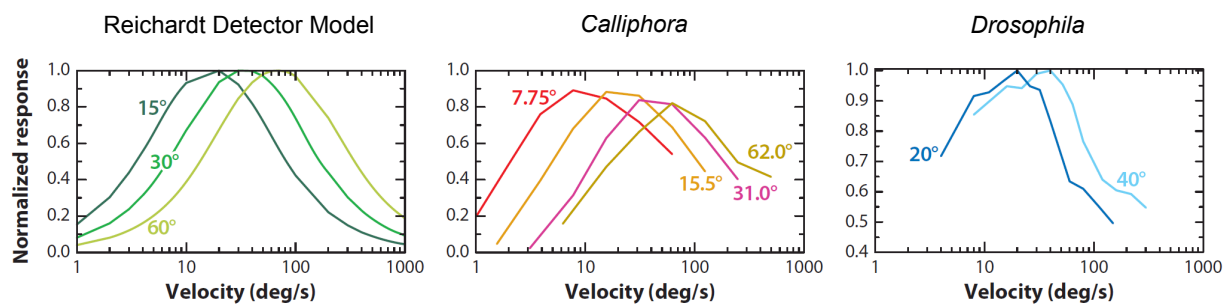


Figure 1.14: Response properties of the Reichardt Detector model and LPTCs.

The three figures depict the responses of simulations of a Reichardt Detector array (left), measurements from LPTCs in *Calliphora* (middle) and *Drosophila* (right). The response to a moving sine grating with fixed wavelength exhibits a specific optimum at an angular velocity depending on the pattern wavelength. (From Borst et al., 2010).

Indeed, a high amount of evidence supporting the Reichardt Detector has been accumulated in the last decades in fly research. Possibly the most striking argument is its response properties as a function of pattern velocity (in $^{\circ}/s$) and wavelength (in $^{\circ}$). For a moving sine grating with fixed wavelength, the response is maximum for a certain velocity as a function of the wavelength; for slower and faster angular velocities, the response decays (Fig. 1.14). This optimum velocity is a linear function of wavelength. Accordingly, there is a unique optimal temporal frequency of the stimulus - also called contrast frequency - the ratio of angular velocity and pattern wavelength (Borst, 2003a) of about 1 - 2 Hz. Indeed, these striking characteristics have been measured in behavioral and electrophysiological experiments across species (Reichardt, 1961; Fermi and Reichardt, 1963; Götz, 1964, 1972; Buchner, 1976; O'Carroll et al., 1996; Haag et al., 2004).

In addition, Riehle and Franceschini (1984) have shown that sequential stimulation of two photoreceptors within the same ommatidium only is sufficient for eliciting direction-selective responses in H1. Also, responses to small field stimulation aimed at activating a small set of EMDs with roughly similar input only are in agreement with theoretical predictions of single EMD responses (Egelhaaf et al., 1989).

Finally, there is evidence that a subtraction process of two direction-selective subunits - as predicted by the two half-detectors - is implemented in the dendrites of LPTCs, by means of excitatory, cholinergic and inhibitory, GABAergic input. This hypothesis is supported by pharmacological experiments with acetylcholine and GABA agonists and antagonists (Egelhaaf et al., 1990; Brotz and Borst, 1996; Single et al., 1997), current injection experiments (Egelhaaf et al., 1990; Gilbert et al., 1991; Borst et al., 1995) and labeling of acetylcholine and GABA receptors (Fig. 1.9; Raghu et al., 2007, 2009).

Enhancing the Reichardt Detector

While the most basic form of the Reichardt Detector is capable of reproducing LPTC and behavioral response characteristics, it usually needs to be modified and extended with proper pre- and post-processing units if specific LPTC responses are to be matched. First, simulated visual input is usually preprocessed in a manner mimicking LMC response properties, that is, removing completely or to a large extent information about the absolute luminance by either providing zero-centered input in the first place, or by convolving the input with a linear band-pass or high-pass filter (Dror et al., 2001; Lindemann et al., 2005; Spavieri et al., 2010). An interesting modeling aspect concerning the preprocessing stage is whether it is necessary to take into account adaptive processes scaling the LMC impulse response to varying luminance

levels, an issue I will elaborate on in the Results chapter.

A further modification to the model, an adaptive high-pass filter in the cross-arms of the detector (Borst et al., 2003) has been proposed to model the contrast-dependence of the so-called after image effect in fly motion vision (Maddess, 1986): The response to a moving grating shows a transient oscillatory component if the grating has been displayed for a sufficient period of time before motion onset (Harris and O'Carroll, 2002; Reisenman et al., 2003), both the amplitude and the decay time constant of these transient oscillations depend on pattern contrast.

Finally, the biophysical properties of the output stage of local motion detectors need to be taken into account when trying to closely match measured data with simulations. A striking difference between predictions by the original model and measurements is reflected in the response of LPTCs to flicker stimuli - that is, stimuli where the brightness of a uniformly illuminated area is increased or decreased. While the two half-detectors of the Reichardt model produce the same response to such stimulation, leading to cancellation at the final subtraction stage and therefore no response, LPTCs respond with a transient increase in activity to such stimuli, the so-called flicker response. This effect can be explained by assuming the two half-detectors are weighed differentially, with the negative half-detector weighed by constant smaller than one (Egelhaaf et al., 1989), or, when modeling conductance-based synapses, by assigning the inhibitory synapses a reversal potential closer to the resting potential than the excitatory synapses (Cuntz et al., 2007; Spavieri et al., 2010). Regardless of the ability to reproduce flicker responses, it may nonetheless be necessary to simulate a conductance based model, i.e. to simulate synaptic conductances in a patch of membrane instead of simply summing up the outputs of an array of motion detectors, to reproduce saturating response characteristics (see e.g. Haag et al., 1992; Weber et al., 2010). Furthermore, for extracellular firing rate measurements as obtained from spiking neurons such as H1, it may be necessary, depending on the required quality of the fit, to take into account the non-linear characteristics of the spiking mechanism, such as refractory period and spiking threshold (Spavieri et al., 2010).

Such modifications to the model usually lead to a significant number of free parameters that need to be adapted to match specific measurements, requiring scanning of a high-dimensional parameter space. In order to tackle this problem, I present a novel method for manual parameter fitting with a MIDI-Controller in the Methods chapter.

ON/OFF Splitting and Its Structural Implications

The final question, and the major focus of this thesis, concerns what can be learnt about the internal structure of the elementary motion detection circuit as implemented in the medulla. The constituting neurons have thus far largely escaped physiological characterization. Therefore, the cells that constitute the motion detection circuit, their connectivity, their biophysical properties and their response properties are still unknown. This situation is about to change with the increasing availability of driver lines for specific candidate cells of the motion detection circuit, combined with genetic tools for silencing, stimulating and imaging neurons.

A particularly interesting question concerns the nature of the non-linear correlation operation, the multiplication. Given that LMCs act to a large extent as high-pass filters, leading to brightness increments encoded as hyperpolarizations and brightness decrements as depolarizations, the multiplication operation needs to be able to multiply positive with positive values (moving OFF edges), negative with negative values (moving ON edges), and, possibly, multiply signals of mixed sign. It is reasonable to assume that this operation is not implemented in a single cell. Rather, it seems plausible that a divide-and-conquer approach is used internally, that is, a biophysically much more plausible multiplication defined for two positive inputs, only. This operation would then be replicated for correlating positive with positive signals, negative with negative signals (after taking their absolute value), and possibly positive with negative signals. The requirement for a sign-correct correlation operation is independent of the question of whether indeed a multiplication is implemented; rather, it poses a challenge for any non-linear correlation operation.

Indeed, such a separation of the visual input into its ON and OFF components has been found by Joesch et al. (2010), later confirmed by Clark et al. (2011). This finding has fundamental sequences for the internal structure of the motion detection circuit by leading to two alternative models based on refining the original Reichardt Detector by incorporating ON and OFF splitting.

The main question arising from the observation that the input is split into ON and OFF components is what the implications of this finding on our knowledge of the motion detection circuit are. Given the success of the original Reichardt Detector, one possibility is to incorporate ON and OFF splitting into the model while retaining its input-output relationship. This reasoning leads to a structure I will refer to as *4-Quadrant-Detector* (Fig. 1.15A). First proposed by Hassenstein and Reichardt in 1956, it consists of four parallel detectors that cover all four possible combinations of input signs (ON-ON, ON-OFF, OFF-ON and OFF-OFF). A 4-Quadrant-Detector is, from its input-output-behavior, mathematically identical to the original

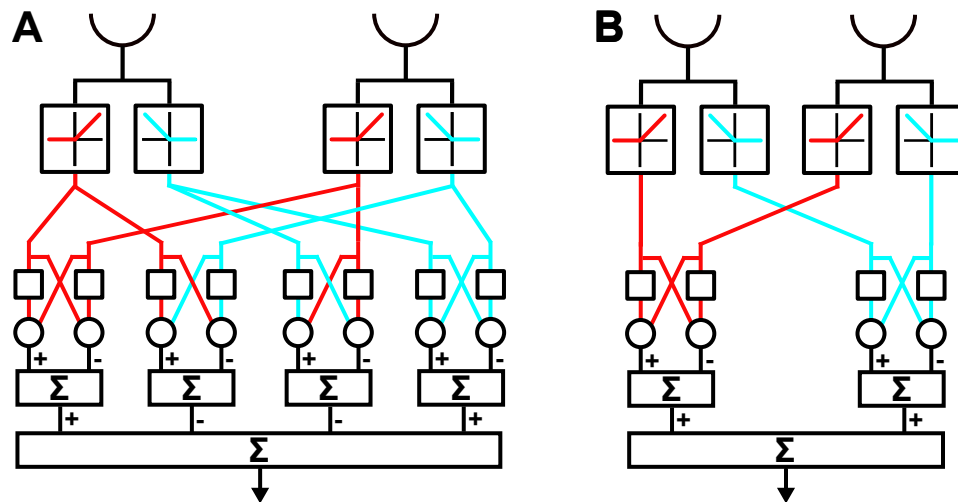


Figure 1.15: Structure of the 4-Quadrant- and the 2-Quadrant-Detector.

The original Reichardt Detector can be refined by incorporating ON and OFF splitting of the input. This leads to two different models. **A** The 4-Quadrant-Detector consists of four identical subunits of the Reichardt Detector type covering all four possible combinations of input signal sign, therefore called 4-Quadrant-Detector. This model is, from its input-output-behavior, mathematically identical to the original Reichardt Detector. **B** The 2-Quadrant-Detector, in contrast, has only two parallel pathways for correlating ON with ON and OFF with OFF signals. It is no longer mathematically equivalent to the original Reichardt Detector since signals of opposite sign do not interact. Both models are biophysically more plausible because both pathways, and therefore the multiplication operations, receive non-negative input signals, only. (Modified from Eichner et al., 2011).

Reichardt Detector. It is biophysically more plausible because the multiplication operations in each subunit are required to work on two positive input values, only.

A second possibility is the so-called *2-Quadrant-Detector* (Fig. 1.15B). This model was first proposed by Franceschini et al. (1989). In a set of impressive experiments, the authors stimulated individually two photoreceptors within one ommatidium with different optical axes and observed direction-selective responses in H1 (Riehle and Franceschini, 1984). Two light beams directed at the different photoreceptors delivered apparent motion stimuli, a sequence of two brightness steps mimicking motion in either H1 preferred or null direction. Direction-selective H1 responses were observed for ON-ON and for OFF-OFF sequences, but not for ON-OFF and OFF-ON sequences. These response properties are in agreement with a 2-Quadrant-Detector where ON and OFF signals from neighboring photoreceptors are not explicitly correlated. Accordingly, and in contrast to the 4-Quadrant-Detector, this model is no longer equivalent to the original Reichardt Detector.

However, a series of experiments performed by Egelhaaf and Borst (1992) challenged the idea of a 2-Quadrant-Detector. Stimulating the fly with apparent motion brightness steps on a CRT monitor, the authors observed responses to ON-ON and OFF-OFF, as well as to ON-OFF and OFF-ON sequences, with the polarity of PD and ND responses inverted for the latter two stimulus sequences. As this thesis will demonstrate, similar results are obtained for a slightly modified stimulus protocol in both *Calliphora* and *Drosophila*, also confirming the results of related studies (Hassenstein, 1951; Tuthill et al., 2011; Clark et al., 2011). By combining experiments and modeling, I try to give a definitive answer to the question whether the fly motion detection circuit is comprised of two or four different pathways, and how these previous measurements can be reconciled with this structure.

Chapter 2

Methods

2.1 Preparation, Electrophysiology and Data Analysis

I recorded extracellular spike trains from the motion-sensitive neuron H1 in 3 - 12 day old blowflies (*Calliphora vicina*) raised in the department stock with a 12h-light-12h-dark cycle. Flies were briefly anesthetized with Carbon Dioxide and fixed with wax. The head capsule was opened, air sacks and fat tissue were removed, then the head was aligned to the frontal pseudo-pupils. I recorded H1 activity with Tungsten electrodes with a resistance of $1M\Omega$ (World Precision Instruments, USA). H1 was identified by its location in the lobula plate, its resting firing rate of 10 - 20 Hz and its characteristic response properties to visual stimuli - excitation by back-to-front motion, and inhibition by front-to-back motion.

The electrode signal was amplified, band-pass filtered and recorded at a sampling frequency of 10 kHz. Further data analysis was performed with MATLAB (MathWorks Inc., Natick, MA). Spikes were detected offline by manually selecting a spike threshold. The average raster (bin size of 0.1 ms) over stimulus repetitions was computed and low-pass filtered with a Gaussian kernel (standard deviation 2.5 ms).

2.2 Stimulus Device

The visual stimulus was presented on a CRT monitor (M21LMAX, Image Systems Corp., USA) updated at 240 Hz and controlled by MATLAB. Gamma correction was performed by first measuring the relationship between the user-controlled pixel value from the interval [0; 1] and the luminance in candela per square meter (cd/m^2) displayed by the monitor, using a Topcon BM-9 luminance meter (Topcon Corp., Japan). With attached shielding in front of the monitor,

it was possible to display luminance values up to 57 cd/m^2 . Desired luminance values were then converted to pixel values by linear interpolation on the previously acquired pixel-value/luminance curve.

The graphics card controlling the CRT monitor was programmed to emit a trigger signal on every frame of the displayed stimulus. This signal was recorded along with the amplified and bandpass-filtered signal from the electrode and allowed for a precise correlation of the stimulus and the measured neural responses.

2.3 Stimulus Protocol and Data Analysis for Contrast and Mean Luminance Dependence

To estimate the relationship between H1 response (firing rate in Hz) and stimulus contrast, I displayed a square wave grating (wavelength $\lambda = 12^\circ$) moving for 35 s with constant angular velocity ($v = 48^\circ/s$) and constant mean luminance, but randomly varied the contrast of the stimulus. The contrast is defined as

$$contrast = \frac{L_{max} - L_{min}}{L_{max} + L_{min}}$$

where L_{min} and L_{max} are the luminance values of the bright and dark stripes of the square wave grating, respectively. The contrast of the stimulus was changed every 50 ms. The contrast values were drawn uniformly from the set $\{0.05; 0.1; 0.15; \dots; 0.85; 0.9; 0.95\}$. This stimulus was presented three times with identical contrast sequences but three different mean luminances, 7.5 cd/m^2 , 15 cd/m^2 and 30 cd/m^2 .

After computing the firing rate averaged over all trials, the contrast-dependency of the H1 response was determined separately for each mean luminance. I first estimated the *latency* between stimulus presentation and H1 response by finding the location of the maximum of the stimulus/response cross-correlation, which was in the range of 16 and 24 ms (the granularity of the stimulus was 4.16 ms due to the monitor refresh rate of 240 Hz). Then, the contrast/response relationship for a specific contrast value c was computed by averaging over all pairs $(c(t); response(t + latency))$.

2.4 Stimulus Protocol for Apparent Motion Stimuli

I stimulated flies with apparent motion stimuli consisting of two horizontally arranged stripes centered at 45° azimuth and 0° elevation. Each stripe had a horizontal extent of 3° and a

vertical extent of 40° . The background luminance was set to 14 cd/m^2 . The luminance of the two stripes was changed in sequence to mimic either front-to-back (ND of H1) or back-to-front (PD of H1) motion.

I used two types of apparent motion stimuli. The first class consisted of a sequence of two luminance steps. An ON step of a stripe refers to a luminance increment of this stripe from the background luminance (14 cd/m^2) to 57 cd/m^2 , while an OFF step is a luminance decrement from 14 cd/m^2 to 1 cd/m^2 . These two brightness steps were temporally separated by a delay of either 1 s or 10 s.

The second class of apparent motion stimuli consisted of a sequence of two luminance pulses instead of persistent luminance steps. The luminance of one stripe was incremented to 57 cd/m^2 (ON pulse) or decremented to 1 cd/m^2 (OFF pulse) for a duration of 16.4 ms, then reset to the background luminance of 14 cd/m^2 . After a delay of 24.6 ms, the luminance of the other stripe was changed, again for a brief period of 16.4 ms.

The luminance values for ON and OFF stimulation were determined by the minimum and maximum luminance that could be emitted by the stimulus device. The background luminance was set to 14 cd/m^2 instead of the medium luminance of the stimulus device (ca. 29 cd/m^2) in order to arrive at approximately similar response amplitudes for either ON or OFF brightness steps.

2.5 Simulations

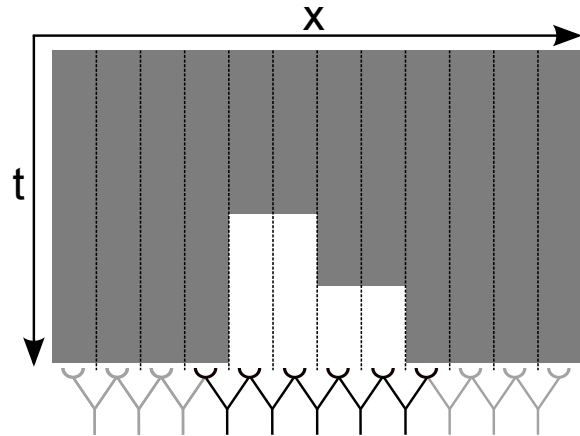
All simulations in this thesis were programmed and run in MATLAB. The motion detector simulations follow a common principle. At the core of all simulations is a function that encapsulates the computation of a motion estimate by a single elementary motion detector based on the original Reichardt Detector. This function takes as input parameters two vectors representing the time-varying stimulus signals arriving at the two photoreceptors, the time step size Δt , and model parameters. The function returns a vector representing the computed time-varying motion estimate. The exact set of parameters for different motion detector models with an input preprocessing stage, and the respective values found during parameter search, are discussed in the next chapter.

The simulations presented in this thesis are usually concerned with the integrated output of an array of motion detectors. In the case of apparent motion stimuli, I summed up the responses of five detectors,

- one detector that observes the left and the right stripe

Figure 2.1: Spatial photoreceptor layout assumption underlying apparent motion simulations.

An array of photoreceptors (bottom, open semicircles) observes an ON-ON brightness step apparent motion stimulus. Each neighboring pair of receptors provides input to one motion detector (bottom, black and gray lines below photoreceptors). Only a subset of these motion detectors is stimulated by the two stripes. In my simulations, I assume five activated motion detectors (depicted in black) and neglect other detectors that are unaffected by the stimulus (gray).



- two detectors that observe only the left, or only the right stripe with both photoreceptors
- two detectors that observe the surrounding area and the left stripe, or the right stripe and the surrounding area, respectively.

These five detectors and the parts of the stimulus they observe are depicted with an x-t-plot in Figure 2.1. Their number and layout is based on the notion that the width of the stripes used in the apparent motion experiments corresponds approximately to one to two times the angular distance between neighboring photoreceptors.

For simulations of an array of detectors that observe a moving sine wave grating, I summed up the responses of 200 motion detectors that covered the whole sine wave period (wavelength $\lambda = 20^\circ$) in a uniform manner. Each detector received input from two photoreceptors separated by an angular distance of $\Delta\phi = 2^\circ$. The two receptors observed the moving stimulus at positions ϕ and $\phi + \Delta\phi$, with $\phi = 0^\circ, 0.1^\circ, 0.2^\circ, \dots, 19.9^\circ$.

For both apparent motion stimuli and moving sine wave gratings, the average luminance was set to 0.3 and the amplitude was set to 0.2 in dimensionless units. Sine wave gratings therefore lied in the range of [0.1; 0.5], and apparent motion stimuli were comprised of ON steps from 0.3 to 0.5 or OFF steps from 0.3 to 0.1.

These simulations were carried out by computing the stimulus (i.e. the two input signals) for a specific motion detector, simulating the response of this detector, and summing up the responses of all 5 or 200 detectors. As an example, I will list the MATLAB code for computing the response of a single Reichardt Detector (angular offset $\phi = 5^\circ$, photoreceptor angular distance $\Delta\phi = 2^\circ$ and low-pass filter time constant $\tau = 0.025s$) to a sine wave grating (wavelength $\lambda = 20^\circ$, amplitude $A = 0.8$ and offset $DC = 1$) moving for 4 s with an angular velocity $v = 20^\circ/s$:

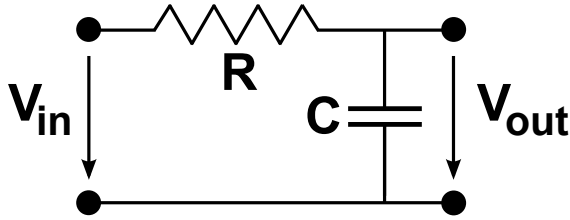


Figure 2.2: An RC-circuit for low-pass filtering.

One way to implement a low-pass filter is a voltage divider consisting of a resistor R and a capacitor C . For a time-varying applied voltage V_{in} , the voltage over the capacitor V_{out} is a low-pass filtered version of V_{in} with time constant $\tau = RC$.

```
dt = 0.001; t = 0:dt:4;
phi = 5; dphi = 2; lambda = 20; v = 40; A = 0.8; DC = 1; tau = 0.025;
in1 = DC + A * sin(2 * pi / lambda * (t * v + phi));
in2 = DC + A * sin(2 * pi / lambda * (t * v + phi + dphi));
r = lowpass(in1, dt, tau) .* in2 - in1 .* lowpass(in2, dt, tau);
```

In the Results chapter, the treated detector models are more complex mainly due to the addition of input preprocessing stages. However, the technical complexity of the source code used for these simulations barely increases. In the following, the implementation of low-pass (as indicated by the `lowpass` function in the above source code example) and high-pass filters will be discussed.

For reasons of simplicity and computational efficiency, I simulated a first-order low-pass filter as implemented by an RC circuit (Fig. 2.2). The voltage drop over the capacitor, V_{out} , is the low-pass filtered version of the input signal. The equation for V_{out} can be derived as follows. First, the current balance equation for the voltage divider consisting of the resistor and capacitor is formulated,

$$I_R = I_C$$

and using $I_R = (V_{in} - V_{out})/R$ and $I_C = C\dot{V}_{out}$ gives

$$\dot{V}_{out} = \frac{1}{RC}(V_{in} - V_{out})$$

In the following, I will replace the voltages with $in := V_{in}$ and $out := V_{out}$ and introduce the time constant $\tau := RC$. The above differential equation can be simulated by applying a truncated Taylor series expansion of the left hand side term, the so-called backward Euler discretization, giving

$$\tau \frac{out(t) - out(t - \Delta t)}{\Delta t} = in(t) - out(t)$$

Solving for $out(t)$ gives

$$out(t) = \frac{\Delta t}{\tau + \Delta t} in(t) + \frac{\tau}{\tau + \Delta t} out(t - \Delta t)$$

The output of a low-pass filter is then computed by iterating over the above equation, starting at $t = \Delta t$ with the initial value $out(0) := in(0)$. To avoid redundant computations, the static parameters $\alpha := \frac{\Delta t}{\tau + \Delta t}$ and $\beta := \frac{\tau}{\tau + \Delta t} = 1 - \alpha$ are computed before starting the iteration, and the actual formula used in the iteration over t is

$$out(t) = \alpha in(t) + \beta out(t - \Delta t)$$

I encapsulated these operations in the above mentioned function `lowpass(in,dt,tau)` where 'in' is a vector of input values at uniformly spaced time points $0, \Delta t, 2\Delta t, \dots$ etc. High-pass-filtering was performed by subtracting the low-pass filtered version of a signal from the signal itself, i.e. `out=in-lowpass(in,dt,tau)`.

2.6 Parameter Fitting

The parameter search for the 2-Quadrant-Detector model presented in the Results chapter was performed with a novel on-line technique. I attached an Evolution UC-33 USB MIDI controller (M-AUDIO/Avid Technology Inc., USA) to the computer performing the simulations, and the positions of its control elements (sliders and knobs) were used by MATLAB to adjust the unknown parameters. The simulation was executed in a loop, repeatedly drawing the newest results on screen, while continuously adjusting the parameters based on the input from the MIDI controller. MATLAB is unable to directly access the MIDI controller; however, it is capable of instantiating Java objects. The latter, in turn, are capable of reading out the position of MIDI control elements via the `javax.sound.midi` application programming interface. I therefore developed a middleware software layer in Java merely serving as a MIDI message buffer between MATLAB and the MIDI controller. This software layer is polled by MATLAB for new messages from the MIDI controller, and parameter values are updated based on observed control element changes.

This method allows to quickly scan a high-dimensional parameter space in order to find a specific solution, e. g. a good quantitative or qualitative fit of a model to some measurement data. Specifically, I determined model parameters of the 2-Quadrant-Detector presented in the next chapter by identifying a parameter set that leads to a good agreement of model simulations with experimentally measured H1 firing rates in response to brightness step apparent motion stimuli.

This method is applicable for parameter fitting in general; however, its major limitation is that the visual feedback to control element changes by plotting the latest simulation results

must have a rather low latency. This limits the applicability of this method to cases where the evaluation of a specific parameter lies below about 0.2 s.

Chapter 3

Results

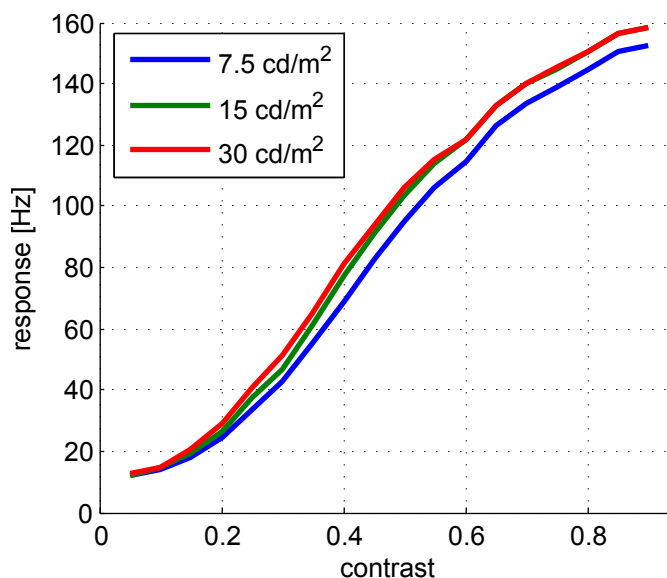
3.1 Response Strength as a Function of Mean Luminance and Contrast

The response amplitude of LPTCs depends strongly on stimulus contrast but seems to be rather independent of the mean luminance (Haag and Borst, 2004). Similar observations have been made at the input level of the motion detection circuit in lamina monopolar cells (LMCs; see Introduction) - the impulse response of LMCs adapts to the mean luminance in such a way that LMCs encode stimulus contrast, not the absolute amplitude of brightness changes in some photometric unit. If this adaptation of the LMC impulse response amplitude to a certain mean luminance level is so fast that it adapts significantly even while a moving grating with constant mean luminance and contrast is shown - i.e. adaptation of the impulse response amplitude to the visible part of the stimulus, either the dark or the bright component of a grating - then it might be necessary to take into account such adaptation in modeling the motion detection circuit. Again, with adaptation to the mean luminance, I do not refer to the high-pass characteristics of LMCs but to the adaptation of the LMC impulse response amplitude to a certain mean luminance level.

To test the dependence of H1 responses in *Calliphora* on contrast and mean luminance, two stimuli were used. First, I estimated the contrast dependence by correlating the response with the stimulus, a square wave grating moving at a constant temporal frequency of 4 Hz and constant mean luminance but rapidly varying contrast (contrast change every 50 ms). This experiment was performed for three different mean luminance levels, 30 cd/m², 15 cd/m², and 7.5 cd/m². As Figure 3.1 illustrates, the response strength shows a strong, slightly

Figure 3.1: H1 response as a function of contrast for different mean luminances.

Correlating the response of H1 (average over 203 stimulus repetitions from eight flies) with the stimulus, a moving square wave grating at a fixed mean luminance but randomly varying contrast reveals a nearly linear relationship between firing rate and contrast. This dependence is largely independent of the mean luminance, indicative for strong adaptation.



saturation dependence on contrast, but is largely independent of the mean luminance. These measurements indicate a strong degree of adaptation of LMC impulse responses but do not reveal the temporal characteristics of the adaptive process.

I therefore applied a second stimulus protocol where a square wave grating was moving at a constant temporal frequency (again 4 Hz) and a constant contrast of 0.9, but the mean luminance was changed every five seconds in the sequence 30 cd/m², 15 cd/m², 7.5 cd/m², 15 cd/m², 30 cd/m². As the contrast dependence measurements in Figure 3.1 revealed, these different mean luminances should result in almost the same response strength after the system has adapted to the new mean luminance. Indeed, this is the case: After a mean luminance decrement, the response strength initially drops but returns to approximately the previous steady state value, with the firing rate following an inverted exponential decay function (Fig. 3.2). The time constant of the adaptation seems to depend on the mean luminance - fitting a function of the form $r - Ae^{-t/\tau}$ (red and green traces in Fig. 3.2) gives two time constants of $\tau = 0.48s$ and $\tau = 0.79s$, respectively. Adaptation after a mean luminance increment is less visible in the response, probably due to saturation of photoreceptor or LMC responses. Note that the overall response strength decays over the period of stimulation due to firing rate adaptation.

As a test whether adaptation shapes the response to such an extent that it needs to be taken into account for the simulations presented in this chapter, I equipped the original Reichardt Detector model with an adaptive preprocessing stage (Fig. 3.3). For each photoreceptor, the input is high-pass filtered with a time constant of 250 ms; the resulting signal is divided by an estimate of the mean luminance, obtained by low-pass filtering the input with a time constant

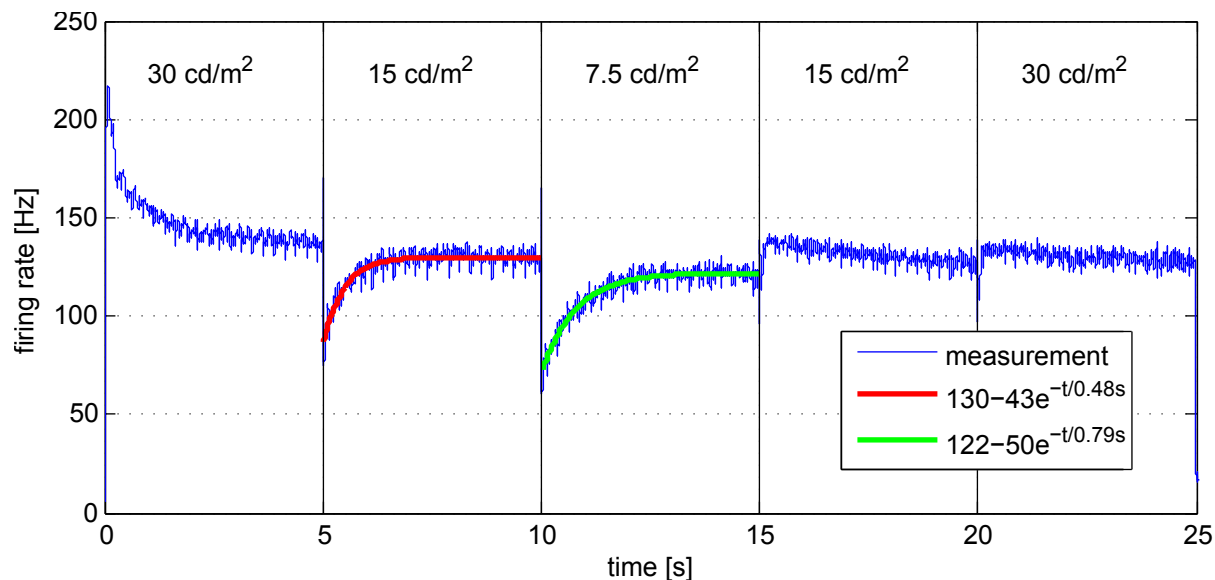


Figure 3.2: Temporal properties of mean luminance adaptation.

A moving square wave grating with constant contrast (0.9) and constant temporal frequency (4 Hz) is displayed for 25 s, with mean luminance changes every 5 s as indicated by the text insets. Upon a luminance decrement, the response (blue trace, average over 203 stimulus repetitions from eight flies) initially drops but returns to approximately the previous steady state value, following a time constant of either 0.48 s (red trace) or 0.79 s (green trace; both are mean squared error fits of an exponential function) depending on the actual luminance step. Adaptation to a brightness increment is barely visible, probably due to saturation of photoreceptors and LMCs.

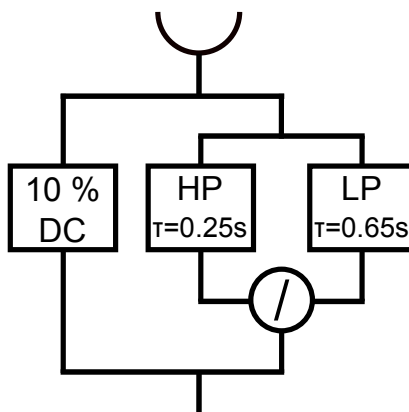
of 650 ms. Then, a 10% fraction of the unfiltered input signal is added to mimic the effect of a DC component.

I then simulated an array of such Reichardt Detectors observing a moving square wave grating at 4 Hz and summed up their responses. To approximate the weak adaptive response characteristics on luminance increments, the preprocessed signal is fed through a saturating function of the form $\tanh(2.25x)$ before being further processed by the motion detectors (omitted from Fig. 3.3; used for simulations in Fig. 3.4, only). To compare the model with the data, the simulation result was scaled by a constant factor, and an offset of 20 Hz mimicking the resting frequency of H1 was added.

Figure 3.4 shows the experimental data (blue) along with the simulation results (red). The initially weaker amplitude of the simulation results (the first five seconds) is likely due to firing rate adaptation of H1 (not incorporated in the simulation), as the experimentally determined response in the last five seconds of the stimulus is weaker than the response to the same mean luminance in the first five seconds. The stronger drop in response strength of the model

Figure 3.3: An adapting LMC model.

The input is high-pass filtered (LP; $\tau = 0.25s$); this signal is then scaled by an estimate of the mean luminance, obtained by low-pass filtering the input (LP; $\tau = 0.65s$). A 10% fraction of the unfiltered input signal is then added to the final output.



for luminance decrements is likely due to the simplified modeling of LMC saturation with the hyperbolic tangent function - better fits can be achieved with appropriately modified saturating functions where brightness decrements are weighed stronger than brightness increments of the same amplitude (data not shown; for contrast-dependency of LMC responses, see Laughlin, 1994).

This model was then used to estimate the influence of adaptation onto the stimuli used in the following sections of this thesis. To facilitate comparison between the LMC models with and without adaption, I omitted the saturating hyperbolic tangent non-linearity in the following simulations (Figs. 3.5 and 3.6).

When a photoreceptor observes a brightness step, LMCs respond with a positive or negative impulse decaying back to, but not entirely reaching, the previous membrane potential with a time constant roughly in the range of 100 ms. Figure 3.5 illustrates simulations of a non-adapting LMC model, where the high-pass filtered input signal ($\tau = 250ms$, blue trace) is added to a 10% DC fraction of the unfiltered input signal. Comparing this response with the adapting LMC model (red trace) reveals that adaptation affects the response, but since the scaling factor is computed by low-pass filtering the input signal, this adaptation affects the response with a certain delay. As a result, the step response of the adapting LMC model does not differ significantly from the non-adapting model except for the decay time constant. In fact, this response can be well approximated by a non-adapting model with a shorter time constant (green trace).

For moving square wave or sine wave gratings with constant mean luminance, the impact of adaptation depends on the temporal frequency of the stimulus. For high temporal frequencies, that is, with periods below the low-pass filter time constant of 650 ms, the mean luminance estimate computed by low-pass filtering the stimulus varies around the actual, constant mean

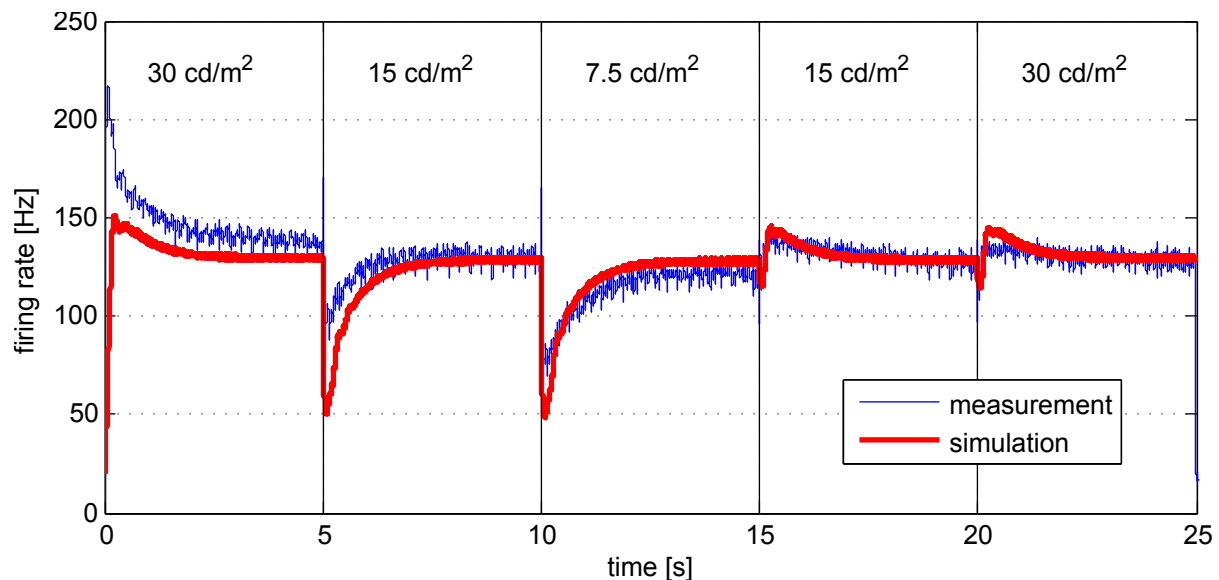


Figure 3.4: Modeling mean luminance adaptation.

The blue trace again depicts the measured response to a square wave grating with fixed contrast and temporal frequency but varying mean luminance, as shown in Figure 3.2. The red trace is the simulated and scaled response of an integrated array of Reichardt Detectors to this stimulus. Each input channel was equipped with an adaptive preprocessing stage as illustrated in Figure 3.3. The output of this preprocessing stage was fed through a saturating non-linearity.

luminance only by a small amount. For very low temporal frequencies, in contrast, the estimated mean luminance approaches the currently visible brightness of the pattern; therefore, adaptation should have a stronger impact on the response. To test these considerations, I simulated responses of the non-adapting and the adapting LMC model as described above for three sine wave stimuli with temporal frequencies of 0.25 Hz, 1 Hz, and 4 Hz, respectively. The results (Fig. 3.6) show that adaptation barely affects the response; it is only distinguishable from the non-adapting model in the case of 0.25 Hz.

In summary, an adaptive LMC model is necessary to reproduce the virtual response invariance to the mean luminance (Fig. 3.2), but does not significantly influence responses to brightness steps or gratings with a constant mean luminance moving at temporal frequencies above approximately 0.5 Hz. In order to reduce the number of free parameters, I therefore decided not to take into account adaptation in the following sections but used a static LMC filter stage instead.

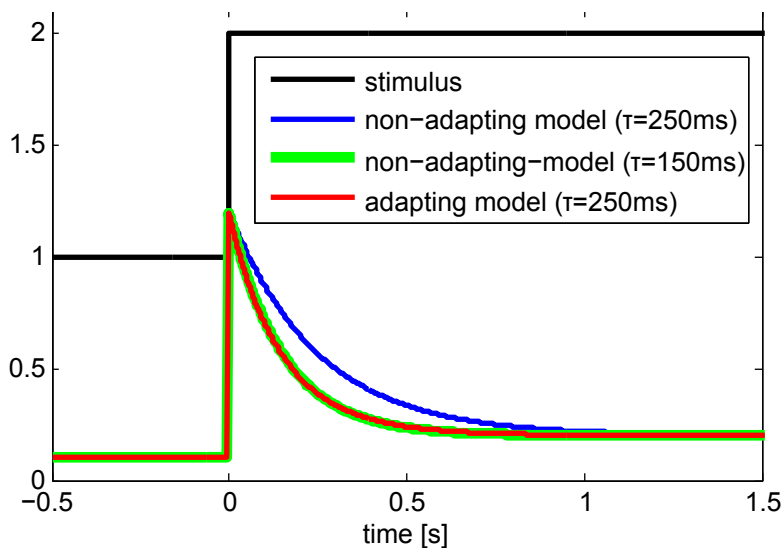


Figure 3.5: Impact of adaptation on brightness step stimuli.

The black trace depicts the stimulus, a brightness step from 1 to 2. The blue trace shows the response of a non-adapting LMC model consisting of 10% of the original signal and the high-pass filtered input ($\tau = 250ms$). An adapting model as presented above shows a similar response (red trace) that is highly similar to the step response of the non-adapting LMC model with a time constant of $\tau = 150ms$. Mean luminance adaptation therefore, according to the model, seems to shape LMC impulse responses only by effectively shortening the decay time constant.

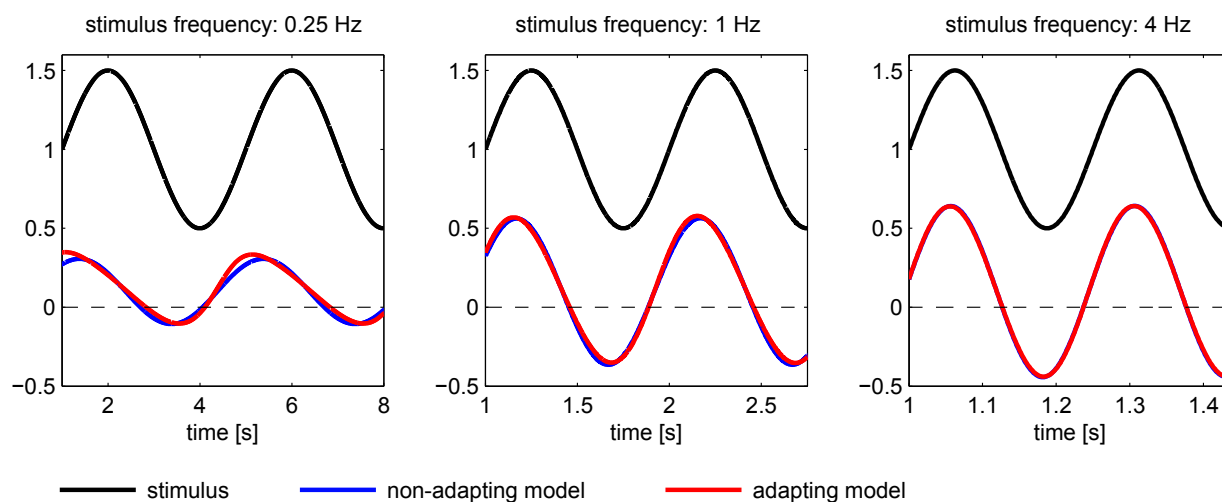


Figure 3.6: Impact of adaptation on sine wave stimuli.

The non-adapting (blue) and the adapting LMC model (red) were stimulated with a sine wave grating (black traces) of 0.25 Hz (left panel), 1 Hz (middle panel) and 4 Hz (right panel). Adaptation shapes the response significantly only for low temporal frequencies.

3.2 Apparent Motion with Brightness Steps

As discussed in the introductory chapter, the finding in *Drosophila* that visual input is split into its ON and OFF components leads to the question whether the motion detection circuit consists of two parallel pathways, correlating only signals of same sign (ON with ON, OFF with OFF) or whether there are four pathways for every combination of input sign (ON-ON, OFF-OFF, ON-OFF, and OFF-ON). It should be possible to decide between these two models, the 2-Quadrant- and the 4-Quadrant-Detector, by using apparent motion stimuli consisting of two spatially displaced, persistent light increment (ON) and decrement (OFF) steps starting from an intermediate luminance, while recording from LPTCs. If direction-selective responses for ON-OFF and OFF-ON sequences are found, this would be an indicator for a 4-Quadrant-Detector.

I performed such experiments in *Calliphora*, recording from H1; Maximilian Joesch performed similar experiments in *Drosophila* while recording from VS cells. The stimulus consisted of two adjacent stripes on a uniformly illuminated background, arranged horizontally for H1 recordings and vertically for VS recordings. The stripe width was set such that the two stripes approximately activated neighboring photoreceptors that form the input to motion detectors. An ON-ON stimulus, for instance, was delivered by first displaying a brightness increment at one stripe, pausing for 1 s, then displaying a brightness increment at the second stripe. The order in which the stripes were activated defines whether the stimulus mimics motion in the cell's preferred or null direction. Figure 3.7A illustrates the stimulus for two horizontally arranged stripes mimicking left-to-right motion for all four possible combinations of brightness steps (ON-ON, OFF-OFF, ON-OFF, OFF-ON).

Figures 3.7B and C illustrate the responses of H1 and VS neurons to such stimuli in PD (red traces) and ND (blue traces). The cells respond to the appearance of the first stripe with an increase in activity, the flicker response, independent of which of the two stripes is activated. The direction-selective property of the motion detection circuit becomes obvious when comparing the PD and the ND response to the appearance of the second stripe. For ON-ON and OFF-OFF sequences (first and second row), the response to PD stimulation is larger than for ND stimulation. However, for ON-OFF and OFF-ON sequences, the response to ND stimulation is larger than for PD stimulation. This effect is called PD-ND inversion. For further illustration, I depict with the black traces the subtraction of the ND responses from the PD responses. The subtracted response is positive for ON-ON and OFF-OFF sequences, but it is negative for ON-OFF and OFF-ON sequences. This observation was made for both

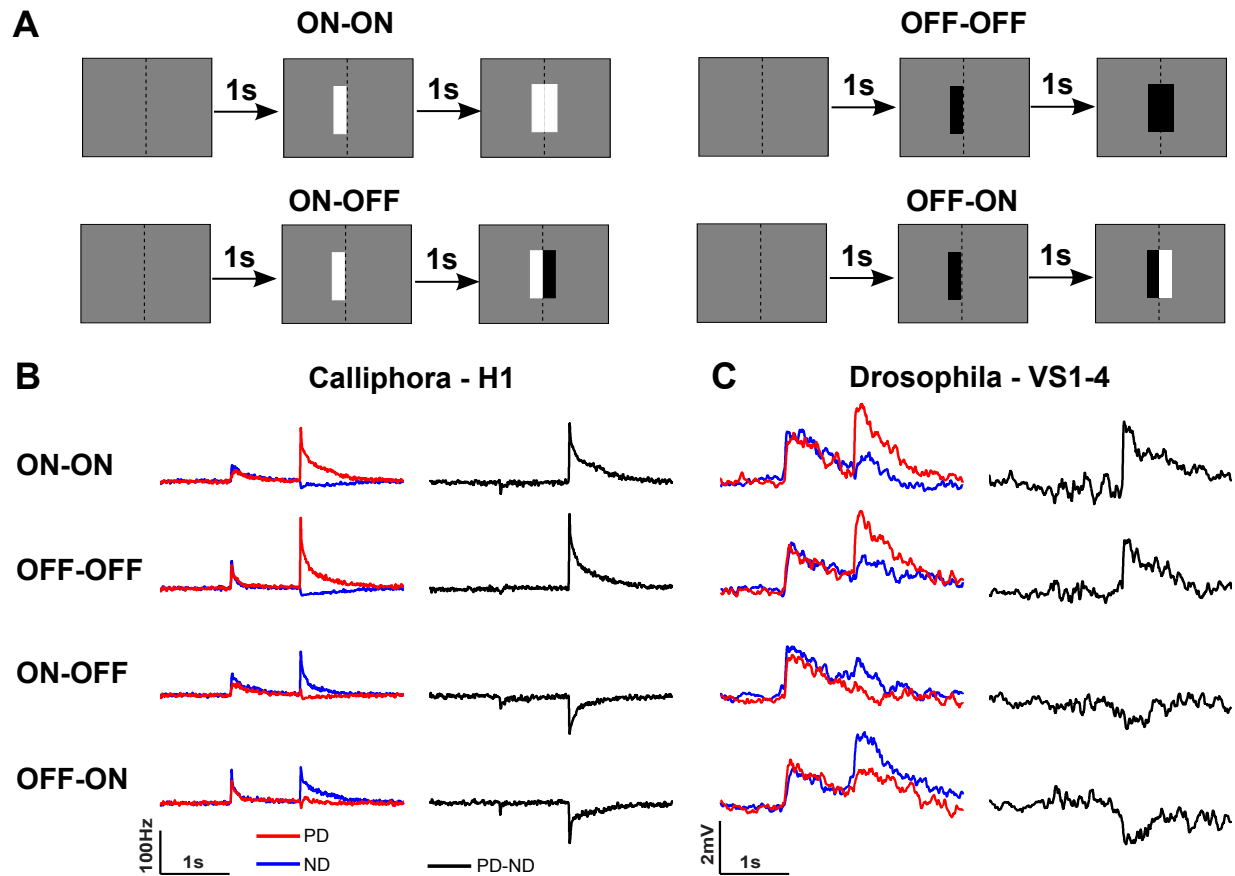


Figure 3.7: Responses of LPTCs to sequences of brightness steps.

A Illustration of apparent motion step stimuli. Two stripes appear in sequence, separated by 1 s, on an intermediate background luminance. Here, only rightward apparent motion is depicted. For the experiments in vertically sensitive VS cells in *Drosophila*, two vertically arranged stripes were used instead. **B** Responses of H1 neurons (average from eight flies) in the blowfly *Calliphora* to apparent motion step stimuli. **C** Responses of VS cells in wild-type *Drosophila* (performed by Maximilian Joesch; average from seven flies). The red traces represent the responses to apparent motion in the cell's preferred direction, the blue traces the responses to apparent motion in the cell's null direction. The black traces represent the difference between the responses to preferred direction and the responses to null direction sequences. For both species, note the positive signals for sequences of same sign (ON-ON, OFF-OFF), and the negative signals for sequences of opposite sign (ON-OFF, OFF-ON). (From Eichner et al., 2011).

experiments in H1 in *Calliphora* and in VS cells in *Drosophila*.

These results, which are in agreement with similar but not identical measurements by Egelhaaf and Borst (1992), at first sight seem to indicate that the structure underlying motion detection is a 4-Quadrant-Detector. First, the 2-Quadrant-Detector, which lacks subunits for correlating ON with OFF stimuli, seems to be incapable of producing direction-selective responses to ON-OFF and OFF-ON sequences. Second, the PD-ND inversion for ON-OFF and OFF-ON sequences seems to be in agreement with the standard Reichardt Detector or its mathematical equivalent, the 4-Quadrant-Detector - the multiplication of two signals with the same sign (ON-ON, OFF-OFF) gives a positive response, while the multiplication of two signals with opposite sign produces a negative response.

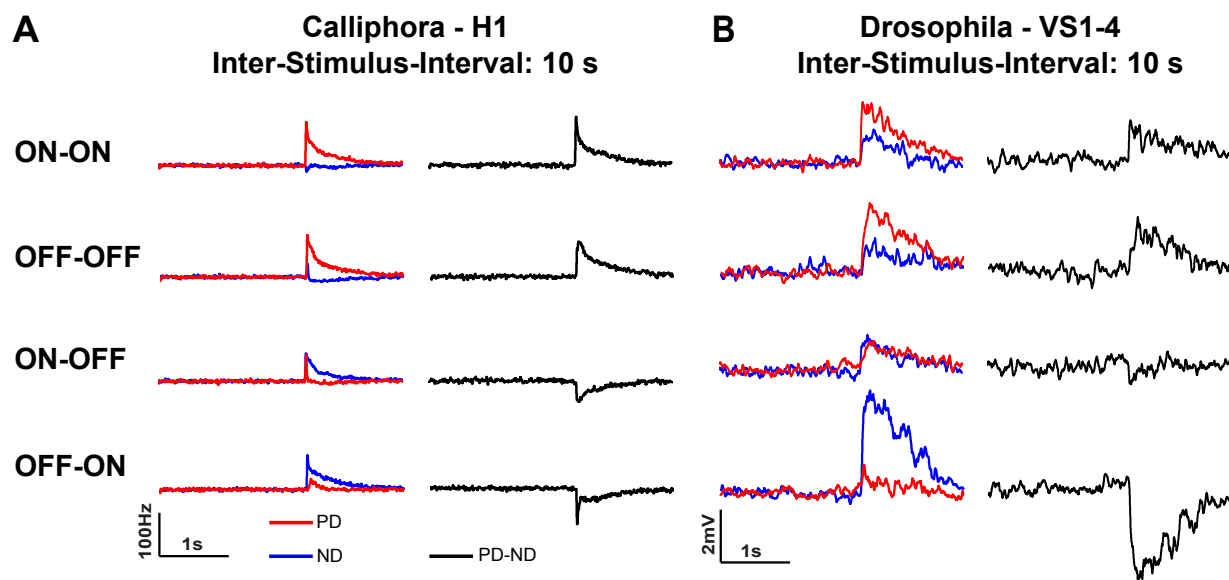


Figure 3.8: Responses of LPTCs to quasi-isolated brightness steps.

In contrast to the stimulus used in Figure 3.7, the first stripe was present for 10 s before the second stripe appeared. The direction selectivity of the response persists in both *Calliphora* (**A**; average from eight flies) and *Drosophila* (**B**; average from seven flies), despite the long separation of the two events. These results show the strong influence of the absolute brightness (DC) on the motion detection system. The experiments in *Drosophila* were carried out by Maximilian Joesch. (From Eichner et al., 2011).

However, it is surprising that the motion detection circuit produces strongly direction-selective responses for inter-stimulus-intervals of 1 s, whereas the low-pass filter time constant of the Reichardt Detector has been estimated to lie between 5 and 50 ms (Guo and Reichardt, 1987; Egelhaaf and Reichardt, 1987; Dror et al., 2001; Borst, 2003a; Lindemann et al., 2005; Spavieri et al., 2010). In fact, the delay between the appearance of the first and the second

brightness step can be increased to at least 10 s without losing the direction-selectivity of the circuit (Fig. 3.8) to all four classes of stimuli, including the PD-ND inversion.

3.3 Simulations and Analytical Treatment

These results provided an important hint: if information about the absolute brightness of a stripe was eliminated in the LMC signal because of pure high-pass filtering, then the appearance of the second stripe after 10 s or more could impossibly lead to direction-selective responses, as the time constant of the low-pass filter is incapable of storing information about the appearance of the first stripe for such extended periods. From the existence of such a directionally selective response, one can conclude that information about the absolute luminance is provided to the elementary motion detector. I accounted for that by adding a DC component (a fraction of the unfiltered input signal) to the output signal of the LMC model. The next step in dissecting the motion detection circuit was then to investigate whether a 2-Quadrant-Detector, equipped with such stimulus preprocessing steps, is capable of reproducing the results presented above.

I therefore designed a modified 2-Quadrant-Detector as depicted in Figure 3.9A. The input, ranging from 0.1 (OFF) to 0.5 (ON), is first preprocessed by a simplified LMC model where a 10% fraction of the original input signal is added to the high-pass filtered ($\tau = 250ms$) version of the input signal. The next stage extracts the ON and the OFF components by half-wave rectification of the preprocessed stimulus. The ON components from the two neighboring input lines are then processed by the ON-ON subunit and the OFF components by the OFF-OFF subunit, with a low-pass filter time constant of 50 ms. For each subunit, the output signals of the two half-detectors are subtracted, with the inhibitory component weighed by a constant of 0.92 relative to the positive output to account for the imbalance between excitatory and inhibitory synaptic input in LPTCs (Egelhaaf et al., 1989). Finally, the signals from both subunits are added up.

Figure 3.9B illustrates the effect of the filter stage and the two half-wave rectifiers. An example stimulus consisting of ON and OFF brightness steps (upper left box) is preprocessed by the LMC model to result in a high-pass filtered version of the original signal, including a small DC component (lower left box, black trace). Due to the positive DC component in this signal, choosing a clip-point of zero for both rectifier stages would result in a smaller OFF component as compared to the ON component; furthermore, such an OFF rectification would remove the DC component from the steady-state OFF signal. Therefore, I shifted the clip-point of the OFF rectifier to 0.05 in order to obtain roughly identical OFF and ON components for

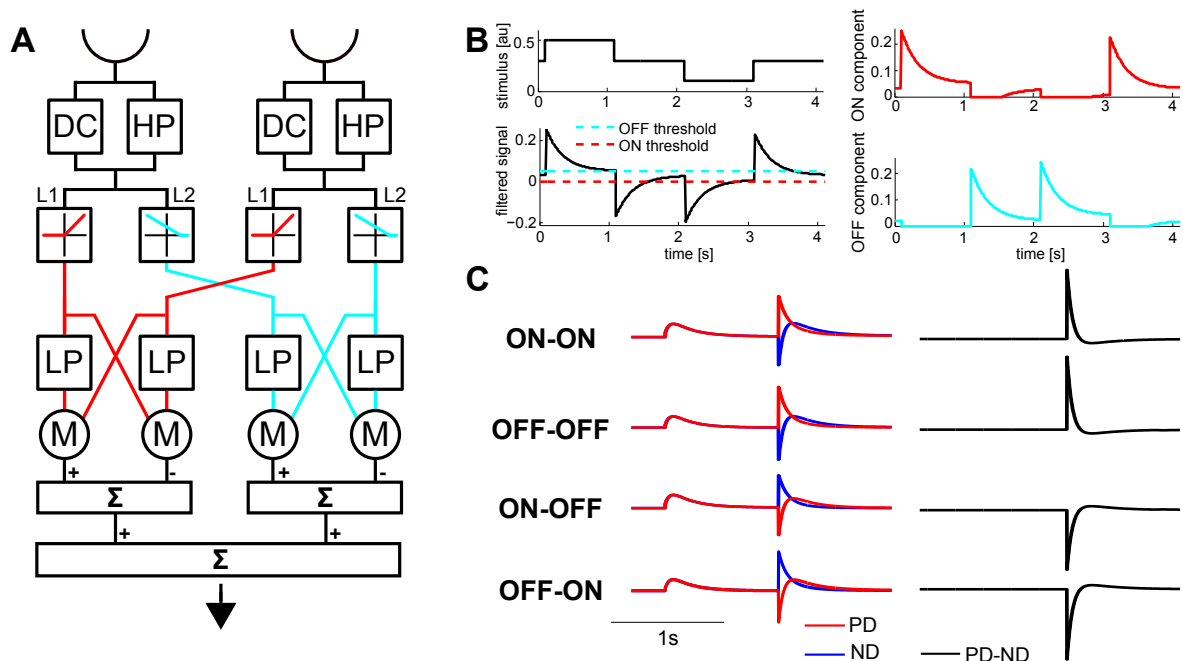


Figure 3.9: Proposed 2-Quadrant-Detector model and its response properties.

A The input is first preprocessed by a filter stage which feeds the signal through a 1st-order high-pass filter (HP, $\tau = 250ms$), but in parallel allows 10% of the original signal to pass (DC). These two signals become added and fed into two parallel half-wave rectifiers that form the input to the ON- (red) and to the the OFF- (blue) pathway, respectively. The cut-off for the ON-rectifier is set to zero. For the OFF-rectifier, it is shifted slightly towards positive signals (exaggerated here for illustration purposes) to account for the observed small ON component in the OFF pathway (Reiff et al., 2010). As for the original Reichardt Detector, the ON and OFF subunits consist each of two 1st-order low-pass filters (LP, $\tau = 50ms$), two multipliers and a subtraction stage. **B** Illustration of ON/OFF extraction by the preprocessing stage depicted in **A**. Upper left panel: example input consisting of a 1 s ON step and a 1 s OFF step. Lower left panel: Resulting signal (black line) after adding up the high-pass filtered stimulus ($\tau = 250ms$) and a 10% fraction of the unfiltered stimulus. Dashed lines: threshold of the ON (red) and OFF (blue) rectifier. Right panels: ON and OFF components extracted by the two rectifiers. **C** Simulated responses of the 2-Quadrant-Detector to apparent motion stimuli. The model exhibits responses similar to the experimental results (compare to Figs. 3.7B and 3.7C): For stimulus sequences of the same sign (ON-ON, OFF-OFF, red traces for preferred direction, blue traces for null direction), the response difference (PD response minus ND response, black traces) is positive, for stimulus sequences of opposite sign (ON-OFF, OFF-ON), the response difference is negative. Until the appearance of the second stimulus, the ND response (blue) is identical to the PD response and therefore covered by the red trace. (Modified from Eichner et al., 2011).

OFF and ON stimuli, respectively. Such a shifted clip-point also accounts for the experimental observation that an ON stimulus leads to a small calcium decrease in the axon terminal of L2, the input neuron to the OFF pathway (Reiff et al., 2010; Joesch et al., 2010). The thresholds for the ON and the OFF pathway are illustrated by the red and blue dashed lines in the lower left panel of Figure 3.9B. The two panels on the right depict the resulting ON (red) and OFF (blue) signal as computed by the rectification stage.

As shown by the experiments with an inter-stimulus-interval of 10 s, LPTC responses to temporally isolated brightness steps are strongly influenced by the brightness of the surrounding area. This consideration implies that the response to a single brightness step is shaped not only by a single detector correlating both stripes with each other but by at least two additional detectors that correlate the surrounding area with the left stripe and the right stripe with the surrounding area, respectively. Therefore, the following simulation results in Figure 3.9C stem not from a single detector but were obtained by integrating over an array of motion detectors as discussed in the Methods section (see Fig. 2.1).

The model comprises a rather large set of free parameters:

- the input range (i.e. values for OFF, intermediate and ON signals processed by the LMC model)
- the high-pass filter time constant of the LMC model
- the DC fraction of the LMC model
- the clip-point of the ON and OFF rectifiers
- the low-pass filter time constants of the ON-ON and OFF-OFF subunits
- the imbalance of the two half-detectors of each subunit

Furthermore, initial simulations comprised other parameters that were later neglected, such as two structurally identical preprocessing stages with different parameter sets for the ON and the OFF detector, respectively, and different weighting of the ON and the OFF detector output. After an exhaustive search of the parameter space aided by a MIDI controller (see Methods chapter), I arrived at a parameter set that gave rise to the simulation results depicted in Figure 3.9C. The model is fully capable of reproducing the experimentally observed response characteristics; it displays direction-selective responses for not only ON-ON and OFF-OFF sequences but also for ON-OFF and OFF-ON sequences, including the PD-ND inversion. This is a remarkable finding since the model lacks explicit ON-OFF and OFF-ON subunits.

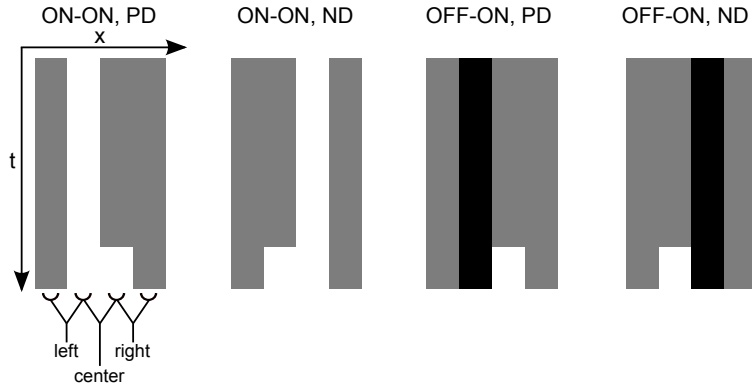
The simulation results constitute a good qualitative fit of the experimental results obtained from *Calliphora* and *Drosophila* (Fig. 3.7B and C). However, several quantitative discrepancies can be observed, most notably stronger ND responses of the simulated model, and different response decay time constants. These differences likely stem from two design choices. First, the model was intentionally kept simple to reduce the number of free parameters and to avoid overfitting. Notable simplifications are the preprocessing stage which is incapable of reproducing the complex temporal response properties of lamina monopolar cells, and the treatment of the output stage as a linear sum of motion detectors instead of a conductance based model with firing rate non-linearities such as spiking threshold and refractory time. Second, I decided to use a single parameter set for fitting the responses from two different fly species (extracellular H1 recordings in *Calliphora* and whole-cell patch-clamp recordings in *Drosophila*) that exhibit different response time constants and flicker response amplitudes.

The finding that the 2-Quadrant-Detector model is capable of reproducing directionally selective responses, including the PD-ND inversion, for ON-OFF and OFF-ON stimuli came as a surprise and is, at first sight, counter-intuitive. After all, this model lacks explicit subunits for correlating ON with OFF signals. In addition, one may well ask whether these response characteristics are a general property of an array of 2-Quadrant-Detectors or valid for a certain, small parameter subspace, only. Therefore, I carried out an analytical treatment of this model to determine the source of direction-selectivity and the PD-ND inversion for ON-OFF and OFF-ON apparent motion sequences. As these response characteristics persist (both in experiments and in the following analytical treatment) for extended time periods two or three orders of magnitude beyond the low-pass filter time constant of the Reichardt Detectors, I calculated the response to the second brightness step of an apparent motion sequence, only. This also allowed me to focus on the ON-ON subunit, only, by computing and comparing the responses to ON-ON and OFF-ON sequences in both PD and ND, respectively.

The four considered stimuli are depicted in Figure 3.10. A second brightness step after a long inter-stimulus-interval is assumed to stimulate two detectors - one correlating the already switched stripe from the first brightness step with the stripe of the second brightness step, the other detector correlating the stripe of the second brightness step with the surrounding area. For ON-ON and OFF-ON PD stimuli, the responses of the center and the right detector were computed; for ND stimuli, I considered the responses of the left and the center detector. The following constant/variable names will be used:

Figure 3.10: Illustration of apparent motion brightness step stimuli with x-t-plots.

From left to right, the following stimuli are depicted: ON-ON PD, ON-ON ND, OFF-ON PD, OFF-ON ND, where PD is defined as motion from left to right. The analytical treatment considers three detectors (left, center, and right), of which two respond to the second brightness step.



$DC_{OFF}, DC_{AVG}, DC_{ON}$ The DC component at the detector input after prolonged display of *OFF*, *AVG* or *ON* luminance

HP_{ON} Time-varying high-pass + DC preprocessor output in response to a brightness step from *AVG* to *ON*

$LP(HP_{ON})$ Time-varying low-pass output in response to a high-pass/DC preprocessed *ON* step

ON-ON_{PD}

First, the individual responses of the center and the right detector are computed:

$$\text{Center detector: } DC_{ON}HP_{ON} - DC_{ON}LP(HP_{ON}) = DC_{ON}(HP_{ON} - LP(HP_{ON}))$$

$$\text{Right detector: } LP(HP_{ON})DC_{AVG} - HP_{ON}DC_{AVG} = DC_{AVG}(LP(HP_{ON}) - HP_{ON})$$

These two responses are summed up, resulting in

$$R(\text{ON-ON}_{PD}) = (DC_{ON} - DC_{AVG})(HP_{ON} - LP(HP_{ON}))$$

ON-ON_{ND}

$$\text{Center detector: } LP(HP_{ON})DC_{ON} - HP_{ON}DC_{ON} = DC_{ON}(LP(HP_{ON}) - HP_{ON})$$

$$\text{Left detector: } DC_{AVG}HP_{ON} - DC_{AVG}LP(HP_{ON}) = DC_{AVG}(HP_{ON} - LP(HP_{ON}))$$

$$R(\text{ON-ON}_{ND}) = -(DC_{ON} - DC_{AVG})(HP_{ON} - LP(HP_{ON}))$$

OFF-ON_{PD}

$$\text{Center detector: } DC_{OFF}HP_{ON} - DC_{OFF}LP(HP_{ON}) = DC_{OFF}(HP_{ON} - LP(HP_{ON}))$$

$$\text{Right detector: } LP(HP_{ON})DC_{AVG} - HP_{ON}DC_{AVG} = DC_{AVG}(LP(HP_{ON}) - HP_{ON})$$

$$R(\text{OFF-ON}_{PD}) = (DC_{OFF} - DC_{AVG})(HP_{ON} - LP(HP_{ON}))$$

OFF-ON_{ND}

$$\text{Center detector: } LP(HP_{ON})DC_{OFF} - HP_{ON}DC_{OFF} = DC_{OFF}(LP(HP_{ON}) - HP_{ON})$$

$$\text{Left detector: } DC_{AVG}HP_{ON} - DC_{AVG}LP(HP_{ON}) = DC_{AVG}(HP_{ON} - LP(HP_{ON}))$$

$$R(\text{OFF-ON}_{ND}) = -(DC_{OFF} - DC_{AVG})(HP_{ON} - LP(HP_{ON}))$$

ON-ON_{PD} - ON-ON_{ND}

Subtracting $R(\text{ON-ON}_{ND})$ from $R(\text{ON-ON}_{PD})$ results in

$$2(HP_{ON} - LP(HP_{ON}))(DC_{ON} - DV_{AVG})$$

with $(DC_{ON} - DC_{AVG}) > 0$

OFF-ON_{PD} - OFF-ON_{ND}

In contrast, subtracting $R(\text{OFF-ON}_{ND})$ from $R(\text{OFF-ON}_{PD})$ gives the same result but with opposite sign, explaining the PD-ND inversion effect:

$$2(HP_{ON} - LP(HP_{ON}))(DC_{OFF} - DC_{AVG})$$

with $(DC_{OFF} - DC_{AVG}) < 0$

Thus, the subtracted responses to ON-ON and to OFF-ON sequences differ in their sign due to the second term that subtracts the two DC components. The first term, $(HP_{ON} - LP(HP_{ON}))$, can be computed analytically. The step response of a high-pass filter (time constant τ_H) plus a DC fraction c is $HP_{ON} = e^{-t/\tau_H} + c, t \geq 0$, and the impulse response of a first-order low-pass filter with time constant τ_L is $\frac{1}{\tau_L}e^{-t/\tau_L}, t \geq 0$. Therefore,

$$HP_{ON} - LP(HP_{ON}) = e^{-t/\tau_H} + c - \int_{t'=0}^t (e^{-t'/\tau_H} + c) \frac{1}{\tau_L} e^{-(t-t')/\tau_L} dt'$$

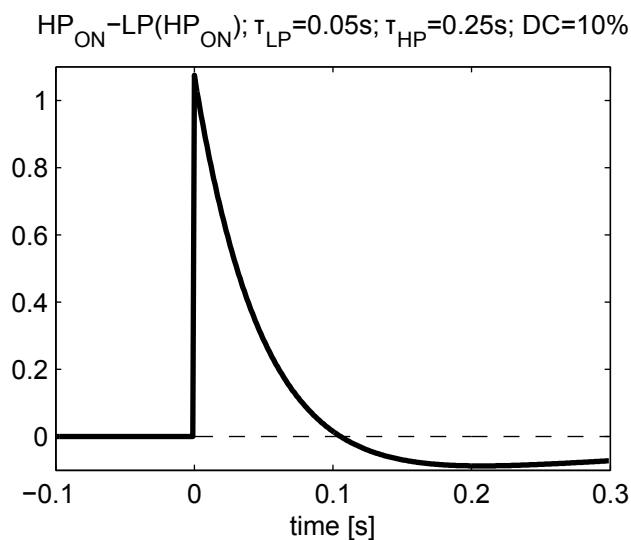
which simplifies to

$$HP_{ON} - LP(HP_{ON}) = \frac{\tau_L}{\tau_L - \tau_H} e^{-t/\tau_H} - \left(\frac{\tau_H}{\tau_L - \tau_H} - c \right) e^{-t/\tau_L}$$

i.e. this term presents the weighted difference of two exponential decays and is thus characterized by a strong positive peak decaying with the low-pass filter time constant and a longer, transient but negative component decaying back to 0 with the high-pass filter time constant. Figure 3.11 illustrates this term for the high-pass and low-pass filter time constants used in the 2-Quadrant-Detector simulations presented in this chapter.

Figure 3.11: Plot of the term $HP_{ON} - LP(HP_{ON})$; $HP_{ON} - LP(HP_{ON}); \tau_{LP}=0.05s; \tau_{HP}=0.25s; DC=10\%$

This figure depicts the time course of the above term in response to a step from 1 to 2 at time $t = 0$ for a low-pass filter time constant of 50 ms and a high-pass filter time constant of 250 ms as used in the previous simulations. The response consists of an initial peak decaying with the low-pass filter time constant, followed by a longer, transient but negative component decaying back to 0 with the high-pass filter time constant.



The 2-Quadrant-Detector is mathematically not identical to the original Reichardt Detector. Thus, the question arises whether this model is able to reproduce experimentally confirmed response characteristics of the Reichardt Detector other than apparent motion stimuli. I therefore performed further simulations with an array of 200 motion detectors, either standard Reichardt Detectors or 2-Quadrant-Detectors, both equipped with the high-pass/DC preprocessing stage illustrated in Figure 3.9A. This array was stimulated by a moving sine wave grating (wavelength of $\lambda = 20^\circ$). First, I compared the response strength as a function of stimulus velocity (Fig. 3.12A). Both models exhibit the characteristic temporal frequency optimum that has been observed experimentally. The only difference is a slightly reduced null direction response of the 2-Quadrant-Detector.

Next, I tested a more subtle response characteristic - the oscillatory component of LPTC responses at the motion onset of a sine grating depends on whether this grating or a uniform gray area is displayed before the grating movement starts. As observed experimentally in LPTCs (Maddess and Laughlin, 1985; Harris and O'Carroll, 2002; Reisenman et al., 2003) and in the original Reichardt Detector (Borst, 2003a), the response of an array of 2-Quadrant-Detectors produces strong initial oscillations when a static grating was presented before motion onset, but only small modulations when instead a uniformly illuminated area is shown (Fig. 3.12B).

Finally, I compared the response properties of the Reichardt Detector array and the 2-Quadrant-Detector array when stimulated with a highly dynamic stimulus, a sine wave grating moving according to a pseudo random velocity profile (Fig. 3.12C; for an example of H1 responses to a similar stimulus, see Spavieri et al., 2010). Both detector models produce an almost identical response to this complex stimulus. In summary, the 2-Quadrant-Detector exhibits the same response characteristics to moving sine wave gratings that have been simulated with the Reichardt Detector and confirmed experimentally.

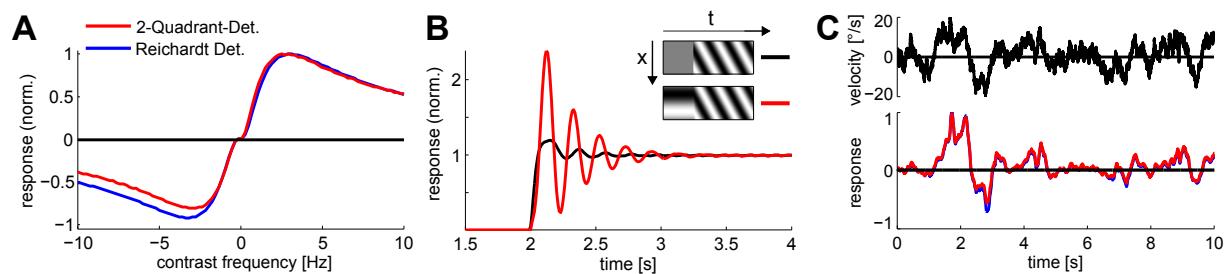


Figure 3.12: Simulations with Reichardt Detector and 2-Quadrant-Detector arrays.

A Normalized steady-state response of an array of standard Reichardt detectors (blue) and 2-Quadrant-Detectors (red) to a moving sine grating (spatial wavelength $\lambda = 20^\circ$) as a function of the temporal frequency of a stimulus. **B** Responses of a spatially integrated array of detectors to the onset of constant grating motion (spatial wavelength $\lambda = 20^\circ$, stimulus velocity $v = 100^\circ/s$) under two conditions: in one case, the grating was visible before the onset of motion (red trace), in the other case the grating was invisible before motion onset (black trace). The detector array exhibits strong oscillations if the grating was visible before motion onset. These oscillations are much weaker if a uniform illumination was shown before the grating started moving. **C** Responses of a spatially integrated array of standard Reichardt detectors (blue) and 2-Quadrant-Detectors (red) to a sine wave grating (spatial wavelength $\lambda = 20^\circ$), moving according to a random velocity profile (low-pass filtered with $\tau = 500ms$) for 10 s. The response of the 2-Quadrant-Detector (red) is largely identical to the response of the Reichardt Detector (blue); therefore, the blue trace is largely covered by the red trace. (Adapted from Eichner et al., 2011).

3.4 Apparent Motion with Brightness Pulses

The simulations and the analytical treatment have shown that the 2-Quadrant-Detector can reproduce the responses to ON-ON, OFF-OFF, ON-OFF and OFF-ON apparent motion sequences based on brightness steps. However, this is not a proof that the internal structure of the fly motion detection circuit is actually comprised of two instead of four pathways: The simulations produce similar or identical results for a 4-Quadrant-Detector. To ultimately distin-

guish between these two models, a different stimulus protocol is needed. The previous section has shown that the PD-ND inversion is produced by a DC component, and that this effect is largely independent of the inter-stimulus-interval. I therefore developed a stimulus protocol that emphasizes the delay-and-correlate mechanism of the Reichardt Detector by using apparent motion stimuli consisting of two short brightness pulses (16ms) instead of brightness steps, separated by a much shorter inter-stimulus-interval of 25 ms (simulations and *Calliphora*) or 48 ms (*Drosophila*). For these stimuli (Fig. 3.13A), the first stripe is no longer visible once the second stripe appears, and direction-selectivity therefore must arise from the delay-and-correlate mechanism. Indeed, it has been shown that apparent motion sequences based on short brightness pulses, in contrast to the previously used brightness steps, do not lead to direction-selective responses for longer inter-stimulus-intervals far beyond the low-pass filter time constant (Egelhaaf and Borst, 1992). It should therefore be possible to determine whether the fly motion detection circuit actually contains subunits for correlating ON with OFF stimuli. The following simulations were performed with the same number of detectors and the same parameter set as used in the previous, brightness step based simulations in Figure 3.9.

In fact, comparing simulations of an array of 4-Quadrant-Detectors (Fig. 3.13B) to an array of 2-Quadrant-Detectors (Fig. 3.13C) in response to stimulation with brightness pulse sequences reveals that direction-selective responses to ON-OFF and OFF-ON stimuli and the PD-ND inversion persist for the 4-Quadrant-Detector but are negligible for the 2-Quadrant-Detector. The corresponding experiments in *Calliphora* (Fig. 3.13D) exhibit strongly direction selective responses to ON-ON and OFF-OFF sequences, but a much weaker effect for ON-OFF and OFF-ON sequences. Similar experiments were carried out in VS cells in *Drosophila* by Bettina Schnell (Fig. 3.13E); however, to avoid overlap of the flicker responses, a longer inter-stimulus-interval of 48 ms was used, and the amplitude of the OFF brightness step had to be increased to obtain significant responses. Again, there is a strong degree of direction-selectivity for ON-ON and OFF-OFF pulse sequences, but not for ON-OFF and OFF-ON pulse sequences. Most importantly, there is no PD-ND inversion for both fly species, as predicted by the 4-Quadrant-Detector.

The responses to ON-OFF and OFF-ON pulse sequences in *Calliphora* are not in perfect agreement with the predictions of the 2-Quadrant-Detector: the subtracted responses are positive. While these results strongly contradict the 4-Quadrant-Detector, they nonetheless constitute a deviation from model predictions. However, the amplitude in response to the second pulse for ON-OFF and OFF-ON sequences varied strongly across flies. The peak subtracted firing rate for ON-OFF sequences amounted to 78 Hz \pm 76 Hz (mean \pm standard deviation

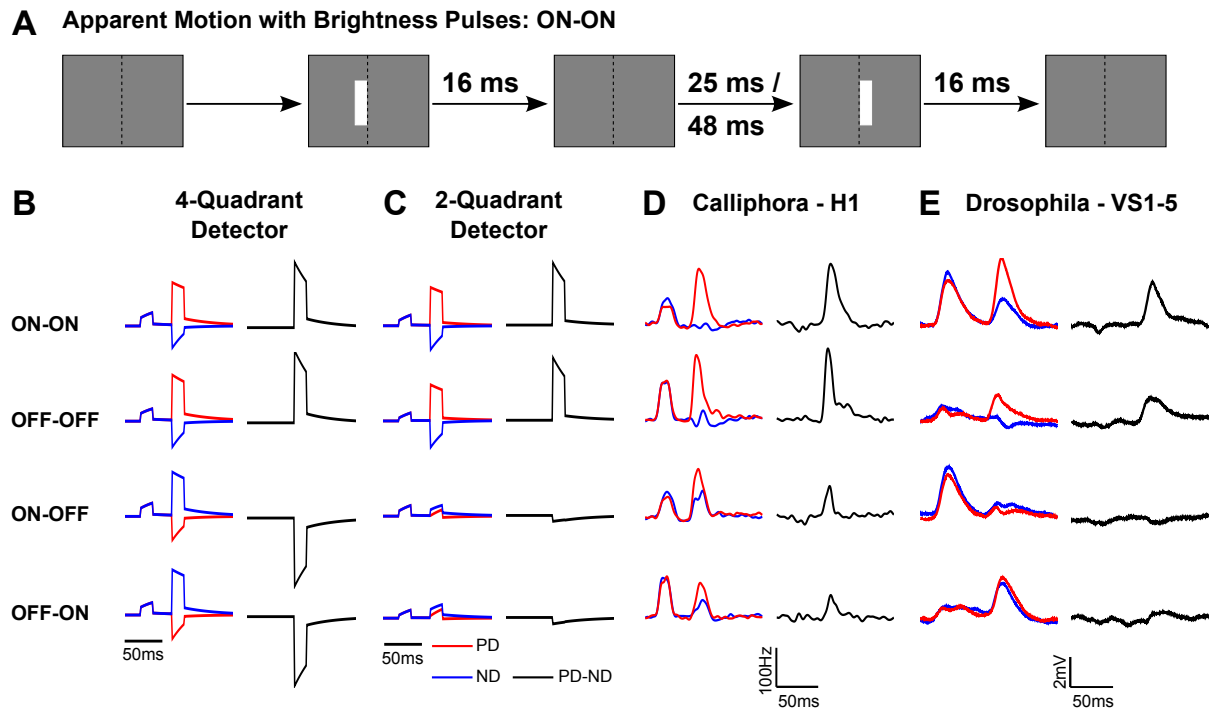


Figure 3.13: Simulations and measurements with brightness pulse based apparent motion stimuli.

Simulations of a 4-Quadrant-Detector, a 2-Quadrant-Detector, and corresponding measurements in *Calliphora* and *Drosophila* for apparent motion stimuli consisting of two brightness pulses. **A** Illustration of an ON-ON PD brightness pulse sequence. Each pulse lasted for 16 ms, and the inter-pulse-interval was 25 ms for *Calliphora* and in the simulations, and 48 ms for *Drosophila*. **B** Simulated responses of the 4-Quadrant-Detector to sequences of brightness pulses. For stimulus sequences of the same sign (ON-ON, OFF-OFF, red traces for preferred direction, blue traces for null direction), the response difference (PD response minus ND response, black traces) is positive. For stimulus sequences of opposite sign (ON-OFF, OFF-ON), the response difference is negative with approximately the same amplitude as for ON-ON and OFF-OFF sequences. **C** Simulated responses of the 2-Quadrant-Detector. For ON-ON and OFF-OFF sequences, the response difference is again positive; for ON-OFF and OFF-ON sequences, the response difference is relatively small. **D** Responses of the H1 neuron in *Calliphora* (average from ten flies). As predicted by both detector types, the response difference to stimulus sequences of same sign is strong, positive and very stable (first and second row; mean response from ten flies). In contrast, the response differences to stimulus sequences of different sign (ON-OFF, OFF-ON; third and fourth row) are rather small and highly variable across flies. **E** Responses of VS cells in *Drosophila* (performed by Bettina Schnell; average from six flies). Responses to ON-ON and OFF-OFF stimuli again give rise to strongly direction-selective responses, while there is no significant difference between PD and ND stimulation with ON-OFF or OFF-ON pulse sequences. These results contradict a 4-Quadrant-Detector scheme underlying motion detection where these stimuli should give a clearly negative response difference. The slight positive response difference in the results from *Calliphora* can be explained by adjusting the input filter parameters of the 2-Quadrant-Detector to result in a more biphasic response of the input stage to brightness pulses. (From Eichner et al., 2011).

across ten flies), and to $56 \text{ Hz} \pm 50 \text{ Hz}$ for OFF-ON sequences. This effect could arise from the biphasic response of LMCs to short brightness pulses (Fig. 1.5; van Hateren, 1992b), leading to slight stimulation of the OFF pathway for ON pulses and vice versa. Indeed, the positivity of the ON-OFF and OFF-ON subtracted responses can be reproduced in simulations by halving the input filter time constants and DC fraction to mimic a more biphasic LMC impulse response (data not shown).

In summary, the simulation results and the experimental data presented in Figure 3.13 clearly refute the 4-Quadrant-Detector as the model underlying motion detection but offer strong support for a 2-Quadrant-Detector as proposed here.

Chapter 4

Discussion

In this thesis, I analyzed the internal structure of the fly motion detection circuit with a combined modeling and electrophysiology approach. I first found that for the stimuli used in this work, adaptive processes that scale the impulse response of the input stage can be neglected. I then found that a model with two parallel, non-interacting circuits for detecting ON and OFF motion, respectively, is in agreement with a wide range of experimental evidence. In contrast, I found that the previous standard model for motion detection cannot explain the lack of responses to ON-OFF and OFF-ON apparent motion stimuli consisting of brief brightness pulses.

4.1 Adaptation of the LMC Impulse Response

For dissecting the insect elementary motion detector, it is important to know how raw luminance signals are preprocessed before they enter the motion detection circuit. In particular, it has been observed that the response amplitude of LPTCs exhibits a strong dependence on stimulus contrast. This phenomenon can, in principle, be explained by a linear filter at the input stage, for instance by convolving the raw input signal with experimentally determined LMC impulse responses. However, the response strength is largely independent of the mean luminance, depending mainly on contrast, when the organism is given enough time to adapt to a given mean luminance. This effect cannot be reproduced by a linear filter with constant amplitude at the input stage - the amplitude of the filter must therefore be adapted to a certain mean luminance, in agreement with experimentally observed adaptation of LMC impulse responses (Laughlin, 1994).

The term mean luminance is defined for a whole grating, however; a single photoreceptor or lamina cartridge are thought to be unaware of the global mean luminance as they observe only a

local region, and therefore specific luminance, of the stimulus. This raises the question whether adaptation of the impulse response amplitude to the locally observed luminance signal shapes LPTC responses in a way that requires it to be taken into account when simulating elementary motion detectors. For instance, LMC impulse responses likely adapt to periodic stimuli with very low temporal frequencies because they observe brightness changes on a long time scale, only; in contrast, the impulse response is likely not subject to adaptation for stimuli with high temporal frequencies. It must be stressed again that such adaptation of the impulse response must not be mistaken with the high-pass characteristics of LMCs that could also be referred to as adaptation to the mean luminance. I therefore estimated the time scale of impulse response adaptation by showing a moving square wave grating with constant contrast but changing mean luminance. The steady state response of H1 to such stimulation is nearly identical, but upon a change of the mean luminance, the response strength also changes before decaying back to the previous steady state value. This adaptive process was found to follow an exponential decay with surprisingly low time constants between 0.5 s and 0.8 s, depending on the new mean luminance.

To test whether this adaptive process shapes the responses to sine wave gratings and brightness steps in a significant manner, I simulated an adaptive preprocessing stage by scaling the high-pass filtered output by an estimate of the mean luminance, obtained from low-pass filtering the raw (time constant of $\tau = 650ms$). An array of Reichardt Detectors equipped with such a preprocessing stage is capable of reproducing the measurements with constant contrast but varying mean luminance. I then used this model to compare simulations of an adapting and a non-adapting preprocessing stage in response to brightness steps and to sine wave stimuli at different temporal frequencies. The results indicate that impulse response adaptation only plays a role for comparatively small temporal frequencies of 0.25 Hz or lower; for brightness steps, adaptation only shortens the decay time constant of the model response, but barely affects its shape. In order to reduce the number of free parameters, I therefore did not incorporate adaptation into the models described in the subsequent sections.

Interestingly, time constants of adaptive processes have been found to depend on stimulus history across species. Fairhall et al. (2001) recorded responses of H1 in *Calliphora* to a moving stimulus with a Gaussian zero-mean white-noise velocity profile. The variance of the underlying distribution was switched between two values σ_1^2 and σ_2^2 every $T/2$ s, with T being the cycle time of the stimulus. Upon a switch of the variance, the response of the recorded cell adapted by adjusting the dynamic response range to the new stimulus statistics. Interestingly, the adaptation time constant depended on the stimulus history in a unique manner: it was nearly

linearly related to the length of the switching cycle T . Wark et al. (2009) arrived at similar results when recording from mouse retinal ganglion cells that were stimulated with a Gaussian white-noise modulated intensity profile. In addition to the aforementioned study, they not only switched between different stimulus standard deviations but also between different mean values (i.e., mean luminance), again finding a linear relationship between switching period and adaptation time constant. Furthermore, the adaptation time constant depended on the magnitude of the parameter change: the bigger the change in variance or mean, the faster adaptation occurred. These findings were well reproduced by a Bayesian inference model where accumulated evidence as represented by the stimulus history is used to estimate the new mean or variance of the stimulus. Although such considerations did not play a role in this thesis, it would be interesting to extend the above analysis to the stimuli presented in the Results chapter, where stimulus velocity, wavelength and contrast were held constant but the mean luminance was varied. One possible experiment would be to alternate between two mean luminances, vary the cycle time and determine whether and in what way the adaptation time constant is affected. A second interesting question concerns how the adaptation time constant depends on both the absolute and the relative magnitude of the mean luminance switch, and how these dependencies could be reproduced by a probabilistic model.

4.2 Four vs. Two Parallel Motion Detectors

Recently, three further studies concerned with preprocessing of visual stimuli before they enter the motion detection circuit have been published. Joesch et al. (2010) found that the lamina monopolar cells L1 and L2 are involved in splitting the input into ON and OFF components. Reiff et al. (2010) performed calcium imaging experiments indicating that OFF splitting takes place directly in L2. Recently published data about similar experiments in L1 indicate that ON splitting does not occur in but postsynaptic to L1, possibly via an inhibitory synapse (Clark et al., 2011). The finding that blocking either L1 or L2 impairs detection of moving ON or OFF edges, respectively, paved the way for the further work presented in this thesis. The most basic question that arose after the finding that input is split into ON and OFF components is whether there exist four or two detector subunits in parallel. The 4-Quadrant-Detector model, consisting of four subunits for each combination of input signs (ON-ON, OFF-OFF, ON-OFF, OFF-ON), is mathematically identical to the original Reichardt Detector and therefore exhibits the same input-output behavior. In contrast, a basic 2-Quadrant-Detector as depicted in Figure 1.15 only correlates inputs of the same sign (ON-ON, OFF-OFF).

4.2.1 Apparent Motion Experiments with Brightness Steps

It seems straightforward to distinguish between these two alternatives: A single detector, or an array of detectors receiving the same input, must be stimulated such that only a specific (hypothetical) subunit is activated. The obvious stimuli to assess these models are apparent motion sequences, comprised of two sequential luminance steps at neighboring locations (ON-ON, OFF-OFF, ON-OFF, and OFF-ON sequences). Then, it should be possible to conclude whether specific ON-OFF or OFF-ON subunits exist by determining if the corresponding stimuli give rise to direction-selective responses. Stimulating single detectors is technically difficult or even impossible. Riehle and Franceschini (1984) used two light beams to stimulate two photoreceptors with different optical axes and applied apparent motion stimuli. This requires a sophisticated optical stimulus device, and it is unclear whether indeed single elementary motion detectors are stimulated: This procedure effectively stimulates two lamina cartridges that form the input to several motion detection units, not only the one stimulated by both lamina cartridges. Nonetheless, using such stimulation, direction-selective responses for ON-ON and OFF-OFF sequences were observed, but not to ON-OFF or OFF-ON sequences (Franceschini et al., 1989).

A technically simpler approach is to display brightness steps with two neighboring stripes on a stimulus device like a monitor or an LED arena, each stripe spanning an angular extent of approximately the inter-ommatidial distance. The idea behind such stimulation is that the two stripes, on average, excite a vertically (for horizontally arranged stripes) or horizontally (for stripes positioned on top of each other) arranged set of neighboring photoreceptors, each forming the input to an elementary motion detector. Applying such stimuli also leads to direction-selective responses for ON-ON and OFF-OFF sequences, but, surprisingly, and in contrast to the measurements by Franceschini et al. (1989), direction-selective responses to ON-OFF and OFF-ON sequences as well. Furthermore, the sign of direction-selectivity to the latter was inverted - ND sequences lead to larger responses than PD sequences - which seemed to be in agreement with theoretical predictions by the Reichardt Detector. Similar observations have been made in the nucleus optic tract of the wallaby (Ibbotson and Clifford, 2001) and in human psychophysics (Anstis, 1970).

At first glance, these observations seem to contradict the 2-Quadrant-Detector: the intuitive understanding of the Reichardt Detector performing a delay-and-multiply operation to detect motion implies that ON and OFF stimuli should be actively correlated in an extra subunit if direction-selective responses for such stimuli are observed. However, the time constant of the low-pass filter performing the delay operation has been estimated to lie between 5 ms and 50

ms (Guo and Reichardt, 1987; Egelhaaf and Reichardt, 1987; Dror et al., 2001; Borst, 2003a; Lindemann et al., 2005; Spavieri et al., 2010). Nonetheless, I observed that direction-selective responses for apparent motion stimuli with brightness steps persist for inter-stimulus-intervals of 10 s or more. This made me reconsider whether a 2-Quadrant-Detector could be reconciled with the aforementioned response properties.

4.2.2 Modeling a Motion Detector with an ON and an OFF Subunit

First, I enhanced the 2-Quadrant-Detector with a stimulus preprocessing stage that high-pass filters the input signal and adds to that a 10% fraction of the original input signal. This inclusion of a DC component in the LMC-like filter stage is supported by electrophysiological characterization of LMC responses. More importantly, a pure high-pass filter at the input stage with a time constant in the range of 100 ms would remove information about the first brightness step after some hundred milliseconds and, thus, cannot explain the existence of direction-selective responses to the second brightness step for inter-stimulus-intervals of 10 s or more.

Second, in my simulations I did not consider the response of a single 2-Quadrant-Detector only. A modified model as described in the previous paragraph gives a response to a temporally isolated brightness step (i.e. for long inter-stimulus-intervals) at one input line, and the amplitude of this response is modulated by the DC component at the other input line. This notion readily implies the second important step: the response is due to not only one detector observing both stripes, but at least two additional detectors that correlate the surrounding area with the left stripe, and the right stripe with the surrounding area, respectively. When simulating not only a single detector but at least three detectors, the 2-Quadrant-Detector model reproduces the experimental findings, that is, direction-selective response for long inter-stimulus-intervals beyond the filter time constants for all four classes of apparent motion sequences, and the PD-ND inversion for ON-OFF and OFF-ON sequences. After performing these simulations, I proved mathematically that these effects are not the consequence of a specific parameter set but present an inherent response property of an array of 2-Quadrant-Detectors under the experimentally verified assumption that the input signal contains a DC component.

The fact that the 2-Quadrant-Detector is able to reproduce experimentally observed responses to ON-OFF and OFF-ON stimulation even for long inter-stimulus-intervals nonetheless did not answer the question whether its internal structure of two parallel, non-interacting pathways is indeed implemented in the fly motion detection circuit. In fact, a 4-Quadrant-Detector equipped with identical preprocessing gives very similar results. A proper understanding of

how the PD-ND inversion arises was key to a novel stimulus protocol that allowed me to finally distinguish between the two models. The initial intuition of how direction-selectivity to ON-OFF and OFF-ON sequences, including the PD-ND inversion, arises was different from the one inferred above - an extra subunit would correlate an ON with an OFF stimulus on a timescale of the low-pass filter time constant. Therefore, it proved conclusive to reduce the inter-stimulus-interval to a value where indeed the two brightness steps are correlated on the basis of the delay-and-multiply paradigm, i.e. to about 25 ms. In addition, it was necessary to remove the influence of the DC component, as this was the crucial point in reproducing the observed responses with the 2-Quadrant-Detector model.

4.2.3 Apparent Motion Experiments with Brightness Pulses

Thus, I presented apparent motion stimuli not based on brightness steps but short, temporally non-overlapping brightness pulses (duration: 16 ms), separated by an inter-stimulus-interval of 25 ms. Indeed, direction-selectivity is limited to inter-stimulus-intervals of about 100 ms when using brightness pulses (Egelhaaf and Borst, 1992), in contrast to the measurements performed with brightness steps. Simulations with either 4-Quadrant-Detectors or 2-Quadrant-Detectors indeed reveal a striking response difference for these stimuli - the 4-Quadrant-Detector again exhibits direction-selectivity and the PD-ND inversion for ON-OFF and OFF-ON sequences, while the 2-Quadrant-Detector responds with only negligible amplitude to ON-OFF and OFF-ON stimuli. The corresponding experiments in *Calliphora* revealed that the measured responses cannot be reconciled with a 4-Quadrant-Detector but match the characteristics of a 2-Quadrant-Detector. Corresponding experiments were then performed in *Drosophila* by Bettina Schnell, showing the same response characteristics as in *Calliphora*. I therefore conclude that the fly motion detection circuit consists of two parallel, non-interacting subunits for detecting ON and OFF motion.

4.3 Outlook

4.3.1 Biophysics of ON and OFF Separation

The principle of splitting visual input into ON and OFF components seems to be an evolutionary conserved feature of early visual systems found in both flies and vertebrates. However, the underlying neural implementations arguably differ. While L1 and L2 in flies seem to respond identically to visual stimuli when recording the membrane potential in their dendrites, in

mammals, the separation of visual input into ON and OFF components is observed already at the synapse between cone photoreceptors and bipolar cells (reviewed in Wässle, 2004). Cones, which respond to ON stimuli with hyperpolarizations and to OFF stimuli with depolarizations, transmit their signal via tonically active synapses by releasing glutamate. However, the post-synaptic bipolar cells express different glutamate receptors, thereby resulting in a class that is excited by ON and a class that is excited by OFF stimulation, respectively.

While these mechanisms are less well understood in flies, most progress towards the cellular and physiological characterization of the motion detection circuit has nonetheless been achieved at this early level of the network. Both L1 and L2 receive inhibitory input from photoreceptors and therefore show similar response properties: in their dendrites, they depolarize in response to OFF stimulation and hyperpolarize in response to ON stimulation. The OFF component could therefore be extracted by voltage gated calcium channels in L2 that allow for calcium influx when the cell depolarizes but remain closed upon hyperpolarizations, effectively performing a half-wave rectification. This hypothesis was strongly corroborated by calcium imaging experiments in L2 axon terminals by Reiff et al. (2010) - the calcium concentration increases upon OFF stimulation, but decreases only slightly upon ON stimulation, hinting towards the presence of a DC component. While calcium signals do not necessarily reflect the membrane potential of a cell, they are indicative for the synaptic output and therefore support the idea of L2 performing an OFF rectification operation.

More complex mechanisms might underly the extraction of the ON component, however. Electrophysiological measurements have shown that ON stimuli are encoded by hyperpolarizations (Laughlin, 1994), and recent calcium imaging experiments in L1 axon terminals also report calcium decreases upon ON stimulation (Clark et al., 2011). Importantly, this study found a much stronger sensitivity of the calcium signal to ON stimulation in L1 than in L2: While in L2, the brightness of the calcium indicator decreases only slightly upon ON steps, L1 responds to both ON and OFF steps with approximately equal amplitude (albeit different sign). One appealing hypothesis for ON extraction is therefore an inhibitory synapse that is active at rest, thereby constantly inhibiting the postsynaptic partner neuron. Upon ON stimulation, L1 hyperpolarizes, leading to closure of voltage-gated calcium channels and calcium depletion from the axon terminals by calcium pumps. The putative inhibitory synapse would therefore become less active or even deactivated, leading to de-inhibition and resulting depolarization of the postsynaptic partner neuron. An OFF stimulus that depolarizes L1 would either have no effect if the synapse operates in its saturation regime when L1 is at rest, or the postsynaptic partner neuron is inhibited even more. In the latter cases, the OFF component could then be

clipped away by a further excitatory synapse. However, these questions remain to be solved by recordings in the postsynaptic partner neurons of L1.

4.3.2 Characterizing the Non-Linearity

An important implication of splitting visual input into ON and OFF components is that the subsequent motion detection circuit now is confronted with non-negative signals only. This significantly facilitates the implementation of the non-linear operation inherent to motion detection (Poggio and Reichardt, 1973). This non-linearity is required to give a positive output for two positive (excitatory) as well as for two negative (inhibitory) inputs. Performing such an operation within one neuron is biophysically implausible. In contrast, splitting the inputs into non-negative signals (ON and OFF) allows for a neural implementation of the non-linearity that operates on two non-negative inputs, only. This unit is replicated for the different signal components with a final stage that combines the outputs.

Nonetheless, this does not answer the question what exact non-linearity is implemented in the fly motion detection circuit. Hassenstein and Reichardt (1956) proposed a multiplication since behavioral experiments (Hassenstein, 1951) showed positive responses for ON-ON and OFF-OFF, but negative responses for ON-OFF and OFF-ON stimuli, reminiscent of a sign-correct multiplicative-like operation. Due to ON and OFF splitting, such a non-linearity needs to operate on non-negative values, only, but leaves open the question whether this non-linear operation indeed corresponds to a 1-Quadrant-multiplication. In general, motion-detection can be performed with a multitude of non-linearities (Grzywacz and Koch, 1987), some of which might impose lower biophysical requirements on a single neuron or neural network than a 1-Quadrant-multiplication does. For instance, I found in simulations that replacing the product of a and b with $(a + b)^2$ does not affect simulation results strongly, while this operation could be implemented quite easily by adding up the two inputs a and b in the dendrites of a cell that then feeds the sum through a super-linear spiking non-linearity.

It is hard to characterize the non-linearity by measuring signals at the output level of the circuit in the lobula plate or even further downstream with behavioral experiments. The input signals (luminance) are likely fed through one-dimensional non-linearities such as threshold operations and saturating functions (see e. g. the saturating contrast-sensitivity curves of LMCs in Laughlin et al., 1987) before they reach the neuron or the neural circuit constituting the required non-linearity. This combined signal may be subject to further non-linearities before it reaches the lobula plate network. Furthermore, a single half-detector with one non-linearity cannot be stimulated in isolation by optical means since the mirror-symmetrical half-detector

receives input from the same pair of photoreceptors. Therefore, further characterization of the non-linear operation used in the motion detection circuit remains highly speculative before the constituting neurons can be characterized in physiological terms.

4.3.3 Identifying and Characterizing the Constituting Neurons

Determining and characterizing the neurons that perform motion detection is an important step towards a full characterization of the circuit. Yet, the complexity of the motion detection network presynaptic to LPTCs might appear discouraging at first sight - for instance, each medulla column contains about 60 different neurons, and new types are still being discovered (Raghu et al., 2011). However, it is safe to assume that only a subset of these neurons is involved in motion detection, while others are involved in color vision or orientation based on polarized skylight.

Among those lamina cells that receive photoreceptor input, L1 and L2 are both necessary and sufficient for motion detection (Rister et al., 2007; Joesch et al., 2010). In contrast, photoreceptor input to L3 is not required, and since it projects to the same layer in the medulla as R8, this cell type has been proposed to be involved in color vision (Anderson and Laughlin, 2000; Rister et al., 2007). These findings do not preclude a role of L4 and L5; in particular, L4 might be involved in motion detection by projecting to two neighboring, more posterior lamina cartridges. Since the core prediction of the Reichardt Detector is the pair-wise correlation of neighboring photoreceptor inputs, this lateral connection might act as neural substrate for a unilateral motion detector (Takemura et al., 2008).

The involved neurons postsynaptic to LMCs are yet unknown, but studying co-stratification allows to identify candidate cell types (Bausenwein et al., 1992) such as Mi1, Tm1 etc. In the lobula plate, there is anatomical evidence that T4 and T5 cells present the output elements of the motion detection circuit (Fischbach and Dittrich, 1989). Both T4 and T5 come in four variants, T4a - T4d and T5a - T5d, with T4a and T5a terminating in the most anterior layer of the lobula plate that is sensitive to front-to-back motion, T4b and T5b terminating in the next layer etc. Such a branching pattern could arise from motion detector circuits with four different preferred directions corresponding to the layers of the lobula plate, where each T4 is the output of an ON and each T5 is the output of an OFF detector. In this case, there would be two types of T4a cells corresponding to the two output lines of the Reichardt Model, one providing inhibitory, one excitatory input to LPTCs.

One approach that has already proven highly successful in the lamina (Strausfeld and Lee, 1991; Meinertzhagen and O'Neil, 1991; Meinertzhagen and Sorra, 2001; Takemura et al., 2008)

is to use electron microscopy to identify the connectivity in the medulla, the lobula and the lobula plate. While this technique has been and will continue to be essential for identifying the neural substrate of the motion detector, it is important to keep in mind that gap junctions cannot be identified with electron microscopy. However, these *electrical synapses* are omnipresent in the fly visual system and play an important part in signal processing. For instance, the gap junction coupling between L1 and L2 proved to be key to explaining the difference in the results obtained by Rister et al. (2007) and Joesch et al. (2010): flies where L1 does not receive input from photoreceptors nevertheless respond to ON motion since L1 receives gap junction mediated input from L2, while blocking the synaptic output of L1 indeed removes responses to ON motion.

Once a candidate neuron has been identified and a highly specific driver line is available, the role of this neuron in the motion detection circuit can be assessed by two means: recording the activity of the cell, either its membrane potential or changes in calcium concentration; or manipulating the cell's activity or output with genetic tools while recording the output signal of the whole circuit. Patch-clamping the somata of columnar neurons is technically highly demanding but principally possible when the cells are labeled with a fluorescent protein. Thus far, successful recordings of Mi1 and Tm2 neurons in response to brightness steps have been performed but not yet published (work by Rudy Behnia; personal communication with Claude Desplan). It remains to be seen whether such measurements can be performed reliably and for other cell types (e. g. T4 or T5) as well. The utility of directly recording a neuron's membrane potential lies in the high temporal resolution of the recording, as opposed to genetically encoded calcium indicators. However, such indicators offer two advantages. First, these experiments are, in principle, easier to perform in small cells than patch-clamping. Second, the actual output signal of a cell, i.e. transmitter release, is well characterized by calcium concentration changes in the axon terminal but may not be reflected well by the membrane potential recorded at the soma or in the dendrites (Reiff et al., 2010; Clark et al., 2011).

A second promising approach is to manipulate the circuit by silencing individual neurons and look at how the motion detector output in LPTCs changes. One possibility is to suppress synaptic output of a candidate neuron by expressing the temperature sensitive dynamin-encoding allele *shibire^{ts}*. Other genetic tools for silencing a neuron include the inward rectifying potassium channel KiR2.1 (Baines et al., 2001) or the photon-activated chloride pump halorhodopsin (Zhang et al., 2007). Equipped with these methods and highly specific driver lines, one might for instance test whether the separation into two motion detectors for ON and OFF is retained up to the lobula plate. In this case, silencing or inhibiting T4 would remove responses to ON

motion but not to OFF motion, and vice versa for T5 cells. As a further example, the role of the lateral L4 projections could be assessed by silencing this neuron and comparing LPTC responses to front-to-back or back-to-front motion.

Applying these genetic tools, however, implies several technical difficulties, often leading to results that are not as unequivocal as desired. One of the biggest impediments is the availability of highly specific driver lines - coexpression of the desired proteins in other cells than the target neuron may lead to unwanted side effects. Furthermore, introducing an alien protein may alter the development of the organism. If unspecific driver lines affect vital cells, a certain gene expression may even lead to lethality. Nonetheless, these tools have already proven highly useful and will continue to play a key role in understanding the task of single neurons in the motion detection circuit.

4.4 Concluding Remarks

The findings in this thesis constitute an important step in the ongoing dissection of the fly motion detection circuit. However, they are concerned with structural aspects of a more general nature. The ultimate goal is to comprehend the circuit on the level of single neurons, that is, to identify the neurons that constitute the motion detection circuit and their connectivity, the function each neuron performs in this circuit, and the biophysical means by which these tasks are performed. However, the circuit remains highly elusive downstream of L1 and L2. Given that up to now, our knowledge is restricted to the anatomy of medulla neurons, one can only speculate about the identity and role of specific cell types. Nonetheless, with expected novel driver lines to target specific candidate neurons, and corresponding genetic tools to silence, activate and record from these cells, the situation looks more promising than ever.

Bibliography

- T. D. Albright, R. Desimone, and C. G. Gross. Columnar organization of directionally selective cells in visual area MT of the macaque. *J Neurophysiol*, 51:16–31, 1984.
- J. C. Anderson and S. B. Laughlin. Photoreceptor performance and the co-ordination of achromatic and chromatic inputs in the fly visual system. *Vision Res*, 40:13–31, 2000.
- S. M. Anstis. Phi movement as a subtractive process. *Vision Res*, 10:1411–1430, 1970.
- R. A. Baines, J. P. Uhler, A. Thompson, S. T. Sweeney, and M. Bate. Altered electrical properties in *Drosophila* neurons developing without synaptic transmission. *J Neurosci*, 21:1523–1531, 2001.
- H. B. Barlow, R. M. Hill, and W. R. Levick. Retinal ganglion cells responding selectively to direction and speed of image motion in the rabbit. *J Physiol*, 173:377–407, 1964.
- B. Bausenwein and K. F. Fischbach. Activity labeling patterns in the medulla of *Drosophila melanogaster* caused by motion stimuli. *Cell Tissue Res*, 270:25–35, 1992.
- B. Bausenwein, A. P. Dittrich, and K. F. Fischbach. The optic lobe of *Drosophila melanogaster*. II. Sorting of retinotopic pathways in the medulla. *Cell Tissue Res*, 267:17–28, 1992.
- W. Bialek, F. Rieke, R. R. de Ruyter van Steveninck, and D. Warland. Reading a neural code. *Science*, 252:1854–7, 1991.
- A. Borst. Models of motion detection. *Nat Neurosci*, 3 Suppl:1168, 2000.
- A. Borst. *Computational Neuroscience: A Comprehensive Approach*, chapter Modeling Fly Motion Vision, pages 397–429. Chapman & Hall/CRC, Boca, Raton, London, New York, Washington D. C., 2003a.

- A. Borst. Noise, not stimulus entropy, determines neural information rate. *J Comput Neurosci*, 14:23–31, 2003b.
- A. Borst. *Drosophila's* view on insect vision. *Curr Biol*, 19:R36–47, 2009a.
- A. Borst. Visual motion models. *Encyclopedia of Neuroscience*, 10:297–305, 2009b.
- A. Borst and S. Bahde. Visual information processing in the fly's landing system. *J Comp Physiol A*, 163:167–173, 1988.
- A. Borst and J. Haag. The intrinsic electrophysiological characteristics of fly lobula plate tangential cells: I. Passive membrane properties. *J Comput Neurosci*, 3:313–36, 1996.
- A. Borst and J. Haag. Neural networks in the cockpit of the fly. *J Comp Physiol A*, 188:419–37, 2002.
- A. Borst, M. Egelhaaf, and J. Haag. Mechanisms of dendritic integration underlying gain control in fly motion-sensitive interneurons. *J Comput Neurosci*, 2:5–18, 1995.
- A. Borst, C. Reisenman, and J. Haag. Adaptation of response transients in fly motion vision. II: Model studies. *Vision Res*, 43:1309–22, 2003.
- A. Borst, J. Haag, and D. F. Reiff. Fly motion vision. *Annu Rev Neurosci*, 33:49–70, 2010.
- E. S. Boyden, F. Zhang, E. Bamberg, G. Nagel, and K. Deisseroth. Millisecond-timescale, genetically targeted optical control of neural activity. *Nat Neurosci*, 8:1263–8, 2005.
- V. Braitenberg. Patterns of projection in the visual system of the fly. I. Retina-lamina projections. *Exp Brain Res*, 3:271–98, 1967.
- A. H. Brand and N. Perrimon. Targeted gene expression as a means of altering cell fates and generating dominant phenotypes. *Development*, 118:401–15, 1993.
- T. M. Brotz and A. Borst. Cholinergic and GABAergic receptors on fly tangential cells and their role in visual motion detection. *J Neurophysiol*, 76:1786–99, 1996.
- E. Buchner. Elementary movement detectors in an insect visual system. *Biol Cybern*, 24:85–101, 1976.
- E. Buchner, S. Buchner, and I. Bülthoff. Deoxyglucose mapping of nervous activity induced in *Drosophila* brain by visual movement. I. Wildtype. *J Comp Physiol A*, 155:471–483, 1984.

- E. K. Buschbeck and N. J. Strausfeld. The relevance of neural architecture to visual performance: phylogenetic conservation and variation in dipteran visual systems. *J Comp Neurol*, 383:282–304, 1997.
- M. Chalfie, Y. Tu, G. Euskirchen, W. W. Ward, and D. C. Prasher. Green fluorescent protein as a marker for gene expression. *Science*, 263:802–5, 1994.
- D. A. Clark, L. Bursztyn, M. A. Horowitz, M. J. Schnitzer, and T. R. Clandinin. Defining the computational structure of the motion detector in *Drosophila*. *Neuron*, 70:1165–1177, June 2011.
- T. Cook and C. Desplan. Photoreceptor subtype specification: from flies to humans. *Semin Cell Dev Biol*, 12:509–18, 2001.
- H. Cuntz, J. Haag, F. Forstner, I. Segev, and A. Borst. Robust coding of flow-field parameters by axo-axonal gap junctions between fly visual interneurons. *Proc Natl Acad Sci USA*, 104:10229–33, 2007.
- R. D. DeVoe. Movement sensitivities of cells in the fly's medulla. *J Comp Physiol A*, 138:93–119, 1980.
- J. K. Douglass and N. J. Strausfeld. Visual motion detection circuits in flies: peripheral motion computation by identified small-field retinotopic neurons. *J Neurosci*, 15:5596–611, 1995.
- J. K. Douglass and N. J. Strausfeld. Visual motion-detection circuits in flies: parallel direction- and non-direction-sensitive pathways between the medulla and lobula plate. *J Neurosci*, 16:4551–62, 1996.
- J. K. Douglass and N. J. Strausfeld. Functionally and anatomically segregated visual pathways in the lobula complex of a calliphorid fly. *J Comp Neurol*, 396:84–104, 1998.
- R. O. Dror, D. C. O'Carroll, and S. B. Laughlin. Accuracy of velocity estimation by Reichardt correlators. *J Opt Soc Am A*, 18:241–52, 2001.
- R. Dubner and S. M. Zeki. Response properties and receptive fields of cells in an anatomically defined region of the superior temporal sulcus in the monkey. *Brain Res*, 35:528–32, 1971.
- M. Egelhaaf. On the neuronal basis of figure-ground discrimination by relative motion in the visual-system of the fly. II. Figure-detection cells, a new class of visual interneurons. *Biol Cybern*, 52:195–209, 1985a.

- M. Egelhaaf. On the neuronal basis of figure-ground discrimination by relative motion in the visual-system of the fly. III. Possible input circuitries and behavioral significance of the FD-cells. *Biol Cybern*, 52:267–280, 1985b.
- M. Egelhaaf and A. Borst. Are there separate ON and OFF channels in fly motion vision? *Visual Neurosci*, 8:151–64, 1992.
- M. Egelhaaf and W. Reichardt. Dynamic response properties of movement detectors - theoretical analysis and electrophysiological investigation in the visual system of the fly. *Biol Cybern*, 56:69–87, 1987.
- M. Egelhaaf, A. Borst, and W. Reichardt. Computational structure of a biological motion-detection system as revealed by local detector analysis in the fly's nervous system. *J Opt Soc Am A*, 6:1070–87, 1989.
- M. Egelhaaf, A. Borst, and B. Pilz. The role of GABA in detecting visual motion. *Brain Res*, 509:156–60, 1990.
- H. Eichner, M. Joesch, B. Schnell, D. F. Reiff, and A. Borst. Internal structure of the fly elementary motion detector. *Neuron*, 70:1155–1164, June 2011.
- Y. M. Elyada, J. Haag, and A. Borst. Different receptive fields in axons and dendrites underlie robust coding in motion-sensitive neurons. *Nat Neurosci*, 12:327–32, 2009.
- T. Euler, P. B. Detwiler, and W. Denk. Directionally selective calcium signals in dendrites of starburst amacrine cells. *Nature*, 418:845–52, 2002.
- A. L. Fairhall, G. D. Lewen, W. Bialek, and R. R. de Ruyter Van Steveninck. Efficiency and ambiguity in an adaptive neural code. *Nature*, 412:787–92, 2001.
- K. Farrow, J. Haag, and A. Borst. Nonlinear, binocular interactions underlying flow field selectivity of a motion-sensitive neuron. *Nat Neurosci*, 9:1312–20, 2006.
- G. Fermi and W. Reichardt. Optomotorische Reaktionen der Fliege *Musca domestica* - Abhängigkeit der Reaktion von der Wellenlänge, der Geschwindigkeit, dem Kontrast und der mittleren Leuchtdichte bewegter periodischer Muster. *Kybernetik*, 2:15–28, 1963.
- K. F. Fischbach and A. P. M. Dittrich. The optic lobe of *Drosophila melanogaster*. I. A Golgi analysis of wild-type structure. *Cell Tissue Res*, 258:441–475, 1989.

- N. Franceschini, A. Riehle, and A. Le Nestour. *Facets of Vision*, chapter Directionally selective motion detection by insect neurons, pages 360–390. Springer, Berlin, 1989.
- S. Gao, S. Y. Takemura, C. Y. Ting, S. Huang, Z. Lu, H. Luan, J. Rister, A. S. Thum, M. Yang, S. T. Hong, J. W. Wang, W. F. Odenwald, B. H. White, I. A. Meinertzhagen, and C. H. Lee. The neural substrate of spectral preference in *Drosophila*. *Neuron*, 60:328–42, 2008.
- G. Geiger and D. R. Nässel. Visual processing of moving single objects and wide-field patterns in flies: Behavioral analysis after laser-surgical removal of interneurons. *Biol Cybern*, 44: 141–149, 1982.
- C. Gilbert, D. K. Penisten, and R. D. DeVoe. Discrimination of visual motion from flicker by identified neurons in the medulla of the fleshfly *Sarcophaga bullata*. *J Comp Physiol A*, 168: 653–73, 1991.
- N. M. Grzywacz and C. Koch. Functional properties of models for direction selectivity in the retina. *Synapse*, 1:417–434, 1987.
- K. G. Götz. Optomotorische Untersuchungen des visuellen Systems einiger Augenmutanten der Fruchtfliege *Drosophila*. *Kybernetik*, 2:77–91, 1964.
- K. G. Götz. Principles of optomotor reactions in insects. *Bibl Ophthalmol*, 82:251–9, 1972.
- K. G. Götz. The optomotor equilibrium of the *Drosophila* navigation system. *J Comp Physiol A*, 99:187–210, 1975.
- A. Guo and W. Reichardt. An estimation of the time constant of movement detectors. *Naturwissenschaften*, 74:91–92, 1987.
- J. Haag and A. Borst. Neural mechanism underlying complex receptive field properties of motion-sensitive interneurons. *Nat Neurosci*, 7:628–34, 2004.
- J. Haag, M. Egelhaaf, and A. Borst. Dendritic integration of motion information in visual interneurons of the blowfly. *Neurosci Lett*, 140:173–6, 1992.
- J. Haag, W. Denk, and A. Borst. Fly motion vision is based on Reichardt detectors regardless of the signal-to-noise ratio. *Proc Natl Acad Sci USA*, 101:16333–8, 2004.
- R. C. Hardie. A histamine-activated chloride channel involved in neurotransmission at a photoreceptor synapse. *Nature*, 339:704–6, 1989.

- R. C. Hardie and P. Raghu. Visual transduction in *Drosophila*. *Nature*, 413:186–193, 2001.
- R. A. Harris and D. C. O'Carroll. Afterimages in fly motion vision. *Vision Res*, 42:1701–14, 2002.
- B. Hassenstein. Ommatidienraster und afferente Bewegungsintegration. *Z Vergl Physiol*, 33:301–326, 1951.
- B. Hassenstein and W. Reichardt. Funktionsanalyse der Bewegungsperzeption eines Käfers. *Naturwissenschaften*, 38:507–507, 1951.
- B. Hassenstein and W. Reichardt. Systemtheoretische Analyse der Zeit, Reihenfolgen und Vorzeichenbewertung bei der Bewegungsperzeption des Rüsselkäfers *Chlorophanus*. *Z Naturforsch Pt B*, 11:513–524, 1956.
- K. Hausen. Motion sensitive interneurons in the optomotor system of the fly. II. The horizontal cells: receptive field organization and response characteristics. *Biol Cybern*, 46:67–79, 1982.
- K. Hausen. *Photoreception and Vision in Invertebrates*, chapter The lobula-complex of the fly: structure, function and significance in visual behaviour. NATO advanced science institutes series. Series A. Plenum Press, New York, 1984.
- K. Hausen and C. Wehrhahn. Microsurgical lesion of horizontal cells changes optomotor yaw responses in the blowfly *Calliphora erythrocephala*. *Proc R Soc Lond B Biol Sci*, 219:211–216, 1983.
- M. Heisenberg and E. Buchner. Role of retinula cell types in visual behavior of *Drosophila melanogaster*. *J Comp Physiol A*, 117:127–162, 1977.
- M. Heisenberg, R. Wonneberger, and R. Wolf. optomotor-blind^{H31} - a *Drosophila* mutant of the lobula plate giant neurons. *J Comp Physiol A*, 124:287–296, 1978.
- R. Hengstenberg. Gaze control in the blowfly *Calliphora*: a multisensory, two-stage integration process. *Semin Neurosci*, 3:19–29, 1991.
- D. H. Hubel. Single unit activity in striate cortex of unrestrained cats. *J Physiol*, 147:226–38, 1959.
- D. H. Hubel and T. N. Wiesel. Receptive fields of single neurones in the cat's striate cortex. *J Physiol*, 148:574–91, 1959.

- M. R. Ibbotson and C. W. Clifford. Interactions between ON and OFF signals in directional motion detectors feeding the not of the wallaby. *J Neurophysiol*, 86:997–1005, 2001.
- M. Järvilehto and F. Zettler. Localized intracellular potentials from pre- and postsynaptic components in the external plexiform layer of an insect retina. *Z Vergl Physiol*, 75:422–&, 1971.
- M. Järvilehto and F. Zettler. Electrophysiological-histological studies on some functional properties of visual cells and second order neurons of an insect retina. *Z Zellforsch Mikrosk Anat*, 136:291–306, 1973.
- M. Joesch, J. Plett, A. Borst, and D. F. Reiff. Response properties of motion-sensitive visual interneurons in the lobula plate of *Drosophila melanogaster*. *Curr Biol*, 18:368–74, 2008.
- M. Joesch, B. Schnell, S. V. Raghu, D. F. Reiff, and A. Borst. ON and OFF pathways in *Drosophila* motion vision. *Nature*, 468:300–4, 2010.
- A. Y. Katsov and T. R. Clandinin. Motion processing streams in *Drosophila* are behaviorally specialized. *Neuron*, 59:322–35, 2008.
- K. Kirschfeld. The projection of the optical environment on the screen of the rhabdomere in the compound eye of the *Musca*. *Exp Brain Res*, 3:248–70, 1967.
- T. Kitamoto. Conditional modification of behavior in *Drosophila* by targeted expression of a temperature-sensitive *shibire* allele in defined neurons. *J Neurobiol*, 47:81–92, 2001.
- H. G. Krapp and R. Hengstenberg. Estimation of self-motion by optic flow processing in single visual interneurons. *Nature*, 384:463–6, 1996.
- H. G. Krapp, B. Hengstenberg, and R. Hengstenberg. Dendritic structure and receptive-field organization of optic flow processing interneurons in the fly. *J Neurophysiol*, 79:1902–1917, 1998.
- T. Labhart and E. P. Meyer. Detectors for polarized skylight in insects: a survey of ommatidial specializations in the dorsal rim area of the compound eye. *Microsc Res Tech*, 47:368–79, 1999.
- M. F. Land and T. S. Collett. Chasing behaviour of houseflies (*Fannia canicularis*). *J Comp Physiol A*, 89:331–357, 1974.

- S. B. Laughlin. Matching coding, circuits, cells, and molecules to signals - general principles of retinal design in the fly's eye. *Prog Retin Eye Res*, 13:165–196, 1994.
- S. B. Laughlin, J. Howard, and B. Blakeslee. Synaptic limitations to contrast coding in the retina of the blowfly *Calliphora*. *Proc R Soc Lond B Biol Sci*, 231:437–467, 1987.
- B. P. Lenting, H. A. Mastebroek, and W. H. Zaagman. Saturation in a wide-field, directionally selective movement detection system in fly vision. *Vision Res*, 24:1341–7, 1984.
- J. P. Lindemann, R. Kern, J. H. van Hateren, H. Ritter, and M. Egelhaaf. On the computations analyzing natural optic flow: quantitative model analysis of the blowfly motion vision pathway. *J Neurosci*, 25:6435–48, 2005.
- T. Maddess. Afterimage-like effects in the motion-sensitive neuron H1. *Proc R Soc Lond B Biol Sci*, 228:433–459, 1986.
- T. Maddess and S. B. Laughlin. Adaptation of the motion-sensitive neuron H1 is generated locally and governed by contrast frequency. *Proc R Soc Lond B Biol Sci*, 225:251–275, 1985.
- M. Mank, A. F. Santos, S. Drenth, T. D. Mrsic-Flogel, S. B. Hofer, V. Stein, T. Hendel, D. F. Reiff, C. Levelt, A. Borst, T. Bonhoeffer, M. Hubener, and O. Griesbeck. A genetically encoded calcium indicator for chronic in vivo two-photon imaging. *Nat Methods*, 5:805–11, 2008.
- I. A. Meinertzhagen and S. D. O'Neil. Synaptic organization of columnar elements in the lamina of the wild type in *Drosophila melanogaster*. *J Comp Neurol*, 305:232–63, 1991.
- I. A. Meinertzhagen and K. E. Sorra. Synaptic organization in the fly's optic lamina: few cells, many synapses and divergent microcircuits. *Prog Brain Res*, 131:53–69, 2001.
- T. Mikeladze-Dvali, C. Desplan, and D. Pistillo. Flipping coins in the fly retina. *Curr Top Dev Biol*, 69:1–15, 2005.
- D. C. O'Carroll, N. J. Bidwell, S. B. Laughlin, and E. J. Warrant. Insect motion detectors matched to visual ecology. *Nature*, 382:63–65, 1996.
- T. Poggio and W. Reichardt. Considerations on models of movement detection. *Kybernetik*, 13:223–227, 1973.

- S. V. Raghu, M. Joesch, A. Borst, and D. F. Reiff. Synaptic organization of lobula plate tangential cells in *Drosophila*: γ -aminobutyric acid receptors and chemical release sites. *J Comp Neurol*, 502:598–610, 2007.
- S. V. Raghu, M. Joesch, S. J. Sigrist, A. Borst, and D. F. Reiff. Synaptic organization of lobula plate tangential cells in *Drosophila*: $D\alpha 7$ cholinergic receptors. *J Neurogenet*, 23:200–9, 2009.
- S. V. Raghu, D. F. Reiff, and A. Borst. Neurons with cholinergic phenotype in the visual system of *Drosophila*. *J Comp Neurol*, 519:162–176, 2011.
- W. Reichardt. *Sensory Communication*, chapter Autocorrelation, a principle for the evaluation of sensory information by the central nervous system, pages 303–317. MIT Press and John Wiley and Sons, New York, London, 1961.
- D. F. Reiff, J. Plett, M. Mank, O. Griesbeck, and A. Borst. Visualizing retinotopic half-wave rectified input to the motion detection circuitry of *Drosophila*. *Nat Neurosci*, 13:973–8, 2010.
- C. Reisenman, J. Haag, and A. Borst. Adaptation of response transients in fly motion vision. I: Experiments. *Vision Res*, 43:1291–307, 2003.
- A. Riehle and N. Franceschini. Motion detection in flies: parametric control over on-off pathways. *Exp Brain Res*, 54:390–4, 1984.
- J. Rister, D. Pauls, B. Schnell, C. Y. Ting, C. H. Lee, I. Sinakevitch, J. Morante, N. J. Strausfeld, K. Ito, and M. Heisenberg. Dissection of the peripheral motion channel in the visual system of *Drosophila melanogaster*. *Neuron*, 56:155–70, 2007.
- C. Schilstra and J. H. van Hateren. Stabilizing gaze in flying blowflies. *Nature*, 395:654, 1998.
- R. Sekuler, S. Anstis, O.J. Braddick, T. Brandt, J.A. Movshon, and G. Orban. *Visual perception: The neurophysiological foundations*, chapter The perception of motion, pages 205–230. Academic Press, San Diego, New York, Berkeley, Boston, London, Sydney, Tokyo, Toronto, 1990.
- S. Single and A. Borst. Dendritic integration and its role in computing image velocity. *Science*, 281:1848–50, 1998.
- S. Single, J. Haag, and A. Borst. Dendritic computation of direction selectivity and gain control in visual interneurons. *J Neurosci*, 17:6023–30, 1997.

- C. Spalthoff, M. Egelhaaf, P. Tinnefeld, and R. Kurtz. Localized direction selective responses in the dendrites of visual interneurons of the fly. *BMC Biol*, 8:36, 2010.
- Jr. Spavieri, D. L., H. Eichner, and A. Borst. Coding efficiency of fly motion processing is set by firing rate, not firing precision. *PLoS Comput Biol*, 6:e1000860, 2010.
- M. V. Srinivasan, S. B. Laughlin, and A. Dubs. Predictive coding: a fresh view of inhibition in the retina. *Proc R Soc Lond B Biol Sci*, 216:427–59, 1982.
- D. G. Stavenga. Insect retinal pigments: spectral characteristics and physiological functions. *Prog Retin Eye Res*, 15:231–259, 1995.
- N. J. Strausfeld. *Atlas of an Insect Brain*. Springer Verlag, Berlin, Heidelberg, New York, 1976.
- N. J. Strausfeld. *Facets of Vision*, chapter Beneath the compound eye: neuroanatomical analysis and physiological correlates in the study of insect vision, pages 317–359. Springer, Berlin, 1989.
- N. J. Strausfeld and U. K. Bassemir. Lobula plate and ocellar interneurons converge onto a cluster of descending neurons leading to neck and leg motor neuropil in *Calliphora erythrocephala*. *Cell Tissue Res*, 240:617–640, 1985.
- N. J. Strausfeld and W. Gronenberg. Descending neurons supplying the neck and flight motor of diptera: organization and neuroanatomical relationships with visual pathways. *J Comp Neurol*, 302:954–72, 1990.
- N. J. Strausfeld and J. K. Lee. Neuronal basis for parallel visual processing in the fly. *Visual Neurosci*, 7:13–33, 1991.
- N. J. Strausfeld and H. S. Seyan. Convergence of visual, haltere, and prosternal inputs at neck motor neurons of *Calliphora erythrocephala*. *Cell Tissue Res*, 240:601–615, 1985.
- N. J. Strausfeld, H. S. Seyan, and J. J. Milde. The neck motor system of the fly *Calliphora erythrocephala*. 1. Muscles and motor neurons. *J Comp Physiol A*, 160:205–224, 1987.
- S. Y. Takemura, Z. Lu, and I. A. Meinertzhagen. Synaptic circuits of the *Drosophila* optic lobe: the input terminals to the medulla. *J Comp Neurol*, 509:493–513, 2008.
- L. Tian, S. A. Hires, T. Mao, D. Huber, M. E. Chiappe, S. H. Chalasani, L. Petreanu, J. Akerboom, S. A. McKinney, E. R. Schreiter, C. I. Bargmann, V. Jayaraman, K. Svoboda, and

- L. L. Looger. Imaging neural activity in worms, flies and mice with improved GCaMP calcium indicators. *Nat Methods*, 6:875–81, 2009.
- J. C. Tuthill, M. E. Chiappe, and M. B. Reiser. Neural correlates of illusory motion perception in *Drosophila*. *Proc Natl Acad Sci USA*, 2011.
- A. M. van der Blik and E. M. Meyerowitz. Dynamin-like protein encoded by the *Drosophila* shibire gene associated with vesicular traffic. *Nature*, 351:411–414, 1991.
- J. H. van Hateren. Real and optimal neural images in early vision. *Nature*, 360:68–70, 1992a.
- J. H. van Hateren. Theoretical predictions of spatiotemporal receptive fields of fly LMCs, and experimental validation. *J Comp Physiol A*, 171:157–170, 1992b.
- J. H. van Hateren. A theory of maximizing sensory information. *Biol Cybern*, 68:23–9, 1992c.
- B. Wark, A. Fairhall, and F. Rieke. Timescales of inference in visual adaptation. *Neuron*, 61:750–761, 2009.
- A. Warzecha and M. Egelhaaf. Response latency of a motion-sensitive neuron in the fly visual system: dependence on stimulus parameters and physiological conditions. *Vision Res*, 40:2973–83, 2000.
- F. Weber, C. K. Machens, and A. Borst. Spatiotemporal response properties of optic-flow processing neurons. *Neuron*, 67:629–42, 2010.
- A. Wertz, B. Gaub, J. Plett, J. Haag, and A. Borst. Robust coding of ego-motion in descending neurons of the fly. *J Neurosci*, 29:14993–5000, 2009.
- R. I. Wilson, G. C. Turner, and G. Laurent. Transformation of olfactory representations in the *Drosophila* antennal lobe. *Science*, 303:366–70, 2004.
- H. Wässle. Parallel processing in the mammalian retina. *Nat Rev Neurosci*, 5:747–757, 2004.
- S. Yamaguchi, R. Wolf, C. Desplan, and M. Heisenberg. Motion vision is independent of color in *Drosophila*. *Proc Natl Acad Sci USA*, 105:4910–5, 2008.
- S. Yamaguchi, C. Desplan, and M. Heisenberg. Contribution of photoreceptor subtypes to spectral wavelength preference in *Drosophila*. *Proc Natl Acad Sci USA*, 107:5634–5639, 2010.

- J. M. Zanker. On the elementary mechanism underlying secondary motion processing. *Philos Trans R Soc Lond B Biol Sci*, 351:1725–36, 1996.
- F. Zhang, L. P. Wang, M. Brauner, J. F. Liewald, K. Kay, N. Watzke, P. G. Wood, E. Bamberg, G. Nagel, A. Gottschalk, and K. Deisseroth. Multimodal fast optical interrogation of neural circuitry. *Nature*, 446:633–9, 2007.
- L. Zheng, G. G. de Polavieja, V. Wolfram, M. H. Asyali, R. C. Hardie, and M. Juusola. Feedback network controls photoreceptor output at the layer of first visual synapses in *Drosophila*. *J Gen Physiol*, 127:495–510, 2006.
- L. Zheng, A. Nikolaev, T. J. Wardill, C. J. O’Kane, G. G. de Polavieja, and M. Juusola. Network adaptation improves temporal representation of naturalistic stimuli in *Drosophila* eye: I Dynamics. *PLoS One*, 4:e4307, 2009.

Acknowledgments

First and foremost, I would like to thank the head of my department and my direct supervisor, Axel Borst. His work on insect motion detection and the Reichardt Detector spans more than 25 years, making him not only the world's expert on this topic but also the scientifically most qualified supervisor one could possibly ask for. He supported me throughout the time of my doctorate in both professional and personal regards. His scientific enthusiasm, writing and presentation skills, deep interest in my work, and strong loyalty make the department possibly one of the best workplaces in neuroscience.

I am also much obliged to Jürgen Haag for sharing his expertise on insect motion vision, discussions, and for teaching me electrophysiology, to Renate Gleich for taking care of the flies, and to Dierk Reiff for discussions, technical help, ski-touring and rock climbing.

My research results would not have been possible without the amazing contributions by Maximilian Joesch and Bettina Schnell. Their landmark work on ON/OFF splitting in *Drosophila* paved the way for my subsequent work, and their suggestions as well as constant inquiries about the state of modeling our experimental data provided a great help and motivation throughout my thesis.

I would like to thank my colleagues throughout the Borst Department for discussions, suggestions and for providing a great work atmosphere, and Andreas Herz and Tim Gollisch for being part of my thesis committee.

Finally, this thesis would not have been possible without the constant support and patience of my friends, Bogdan, Franz, Hansi, Nils, Friedrich, Marion, Armin, and my parents, Hanni and Simon.

Curriculum Vitae

Hubert Georg Eichner, born November 4th, 1981 in Bad Reichenhall, Germany

Education

- 2008 - 2011 **Max-Planck-Institute of Neurobiology, Martinsried, Germany**
Ph.D. student, Department of Systems and Computational Neurobiology
Supervisor: Prof. Dr. Alexander Borst
Subject: Internal Structure of the Fly Elementary Motion Detector
- 2001 - 2007 **Technical University Munich**
Diplom-Informatiker (univ.), summa cum laude
Supervisor: Prof. Dr. Arndt Bode
Subject: Parallelization of Biophysically Realistic Neural Simulations
on Multi-Core Architectures

Courses

- 08/2009 Student in *Methods in Computational Neuroscience*
Marine Biological Laboratory, Woods Hole, MA

Publications

- Eichner, H., Joesch, M., Schnell, B., Reiff, D. F., and Borst, A. Internal Structure of the Fly Elementary Motion Detector. *Neuron*, 70(6):1155-1164, 2011.
- Spavieri, D. L., Eichner, H., and Borst, A. Coding Efficiency of Fly Motion Processing Is Set by Firing Rate, Not Firing Precision. *PLoS Computational Biology*, 6(7):e1000860, 2010.

- Eichner, H., Klug, T., and Borst, A. Neural simulations on multi-core architectures. *Frontiers in Neuroinformatics*, 3, 2009.
- Hines, L. M., Eichner, H., and Schürmann, F. Neuron splitting in compute-bound parallel network simulations enables runtime scaling with twice as many processors. *Journal of Computational Neuroscience* 25:203-210, 2008.
- Weber, F., Eichner, H., Cuntz, H., and Borst, A. Eigenanalysis of a neural network for optic flow processing. *New Journal of Physics*, 10, 2008.
- Eichner, H., Trinitis, C., and Klug, T. Implementation of a DSM-System on Top of InfiniBand. Special Session on "Parallel and Distributed Storage Systems" at 14th Euro-micro International Conference on Parallel, Distributed and Network-based Processing (PDP2006), Montbeliard-Sochaux, France (2006).

Employment and Teaching

08/2011	Teaching Assistant for <i>Methods in Computational Neuroscience</i> Marine Biological Laboratory, Woods Hole, MA
05/2009, 05/2010	Teaching Assistant for Practical Course <i>Animal Physiology</i> Ludwig-Maximilians-Universität München, Faculty of Biology
10/2008 - 02/2009	Teaching Assistant for Lecture <i>Computational Neuroscience</i> Ludwig-Maximilians-Universität München, Faculty of Biology
05/2006 - 02/2008	Student Assistant Department of System and Computational Neurobiology Max-Planck-Institute of Neurobiology
07/2005 - 09/2005	Participation in the <i>Extreme Blue</i> internship program Project: <i>InfiniBand Onloading for Microprocessors</i> Department: Logic Design IBM Deutschland Entwicklung GmbH, Böblingen
12/2004 - 07/2005, 02/2006 - 06/2006	Student Assistant System Administrator for the InfiniBand Linux Cluster Lehrstuhl für Rechnertechnik und Rechnerorganisation / Parallelrechnerarchitektur

Technical University Munich, Faculty of Computer Science

08/2004 - 09/2004 Programmer
Implementation of a database loading utility for parsing
text files with freely configurable format
Transaction Software GmbH, München

08/1999, 11/1999 Quality Assurance
OneVision AG, Regensburg

Other

09/2010 Talking Science with Karel Svoboda
Organizer

06/2009 Talking Science with Markus Meister
Organizer

12/2008 Siemens Preis for Diploma Thesis

Language Skills

Fluent in German and English, conversational level Spanish, rudimentary French

Versicherung

Ehrenwörtliche Versicherung

Ich versichere hiermit ehrenwörtlich, dass die vorgelegte Dissertation von mir selbstständig und ohne unerlaubte Hilfe angefertigt ist.

München, den 30.09.2011

Hubert Eichner

Erklärung

Hiermit erkläre ich, dass die Dissertation nicht ganz oder in wesentlichen Teilen einer anderen Prüfungskommission vorgelegt worden ist und dass ich mich anderweitig einer Doktorprüfung ohne Erfolg nicht unterzogen habe.

München, den 30.09.2011

Hubert Eichner